Report No. BC-353-27

EXPERIMENTAL INVESTIGATION AND ANALYSIS OF FLOW UNDER BARRIER WALLS

submitted to

The Florida Department of Transportation

by the

Department of Civil and Environmental Engineering
College of Engineering
University of South Florida
Tampa, Florida, 33620
Ph. (813) 974-2275
February 18, 2005

FINAL REPORT

prepared for the

FLORIDA DEPARTMENT OF TRANSPORTATION

and the

U.S. DEPARTMENT OF TRANSPORTATION
FEDERAL HIGHWAY ADMINISTRATION

Technical Report Documentation Page

1. Report No.	2. Government Accession No.	3. Recipient's Catalog No.
FL/DOT/RMC/ BC-353-27		

4. Title and Subtitle	5. Report Date
EXPERIMENTAL INVESTIGATION AND ANALYSIS OF FLOW UNDER BARRIER WALLS	FEB, 2005
	6. Performing Organization Code FL/DOT
7. Author(s) KRANC, SC. et al	8. Performing Organization Report No.
9. Performing Organization Name and Address Department of Civil and Environmental Engineering ENB118 University of South Florida Tampa, FL 33620	10. Work Unit No. (TRAIS)
	11. Contract or Grant No. BC353 RPWO #27
12. Sponsoring Agency Name and Address **Florida Department of Transportation** **605 Suwannee St. MS 30** **Tallahassee, Florida 32399** **(850)414-4615**	13. Type of Report and Period Covered **Final Report** 7/01-2/05
	14. Sponsoring Agency Code

15. Supplementary Notes

Prepared in cooperation with the USDOT and FHWA

16. Abstract

This report details a performance analysis for flow through inertial attenuators currently used by the Florida Department of Transportation for pavement drainage. Experiments were conducted using full size models of one inlet configuration (Index 415 barrier) and empirical relationships for capacity were derived. A computational model for system design was formulated from this information.

17. Key Word	18. Distribution Statement
Drainage, Barriers, Stormwater	**No Restriction** **This report is available to the public through the NTIS, Springfield, VA 22161**

19. Security Classif. (of this report)	20. Security Classif. (of this page)	21. No. of Pages	22. Price
Unclassified	**Unclassified**	51	

Report No. BC-353-27

EXPERIMENTAL INVESTIGATION AND ANALYSIS OF FLOW UNDER BARRIER WALLS

submitted to

The Florida Department of Transportation

by the

Department of Civil and Environmental Engineering
College of Engineering
University of South Florida
Tampa, Florida, 33620
Ph. (813) 974-2275
February 18, 2005

FINAL REPORT

prepared for the

FLORIDA DEPARTMENT OF TRANSPORTATION

and the

U.S. DEPARTMENT OF TRANSPORTATION
FEDERAL HIGHWAY ADMINISTRATION

EXPERIMENTAL INVESTIGATION AND ANALYSIS OF FLOW UNDER BARRIER WALLS

S. C. Kranc, Ph.D., P.E.
Principal Investigator

with

Christopher J. Cromwell and Clayton J. Rabens
Nathan Collier and Bryan Fast

Department of Civil and Environmental Engineering
College of Engineering
University of South Florida
Tampa, Florida, 33620
March, 2003

TABLE OF CONTENTS

Nomenclature	ii
Conversion Factors	iii
Summary	iv
Introduction	1
Experimental Facility and Observational Methods	4
Measurement of Inlet Capacity	7
Other Complicating Factors	11
Model Development	14
Flow Relationships	16
Detailed Analysis of Flow Conditions on Grade	17
Spreadsheet Model for Design	26
Worksheets	28
Computing the Pond Depth	31
Instructions for Data Entry	32
Example Calculation	33
Comparisons between Detailed Program and Spreadsheet	37
Conclusions	39
References	40
Appendix A: Notes to Accompany Spreadsheet Software	41
Appendix B: Flow in Gutters and Inlets	42
Appendix C: Scaling Relationships	45
Appendix D: An Approximate Model for the K-Barrier	46
Appendix E: Composite Slopes	48
Appendix F: Development of a Visual Basic© Program	50

NOMENCLATURE

In this report, dimensions are given in English units. If no units are given then the quantity is nondimensional.

A = area, (ft^2)
b = length of attenuator, (ft)
B= depth of attenuator, (ft)
C_{DW} = weir discharge coefficient
C_{DO} = orifice discharge coefficient
e = efficiency
E= specific energy, (ft)
Fr= Froude Number
g = acceleration of gravity, (ft/s^2)
h= depth of flow, (ft)
H= height of inlet, (ft)
k = constant in Manning's equation (dimensional conversion)
l_p,l_m = model and prototype dimensions, (ft)
L =length of inlet aperture, (ft)
L = characteristic dimension, (ft)
L_r = characteristic length ratio
n= Manning's n
Q = flow rate, (ft^3/s)
R_h = hydraulic radius, (ft)
S_o = longitudinal slope
S_c = cross slope
T = spread measured across pavement, (ft)
V = velocity, (ft/s)
w = width, (ft)
y = depth of flow, (ft)

CONVERSION FACTORS

To convert	British	SI	multiply by
Acceleration	ft/s^2	m/s^2	3.048E-1
Area	ft^2	m^2	9.290E-2
Density	$slugs/ft^3$	kg/m^3	5.154E+2
Length	ft	m	3.048E-1
Pressure	lb/ft^2	N/m^2	4.788E+1
Velocity	ft/s	m/s	3.048E-1
Volume flowrate	ft^3/s	m^3/s	2.832E-2
Volume flowrate	gal/min	l/s	6.310E-2

CONSTANTS

Acceleration of gravity	32.19 ft/s^2	9.81m/s^2
Density of water	1.94 $slugs/ft^3$	1000 kg/m^3
Manning's constant	1.485	1.0

SUMMARY

Problem statement

Temporary concrete barriers (inertial attenuators) are often installed at highway construction sites, on the edge of driving lanes for traffic safety. To permit pavement drainage, cutouts are included at the bottoms of the barriers to form a small rectangular drainage inlet when the barrier is placed on the pavement. Because these barriers rest directly on the pavement or shoulder, a hydraulic configuration much like a curb and gutter is created. While runoff from the pavement is usually a continuous distribution, these inlets are located at regular, closely spaced intervals, due to the positioning of the barriers. In this regard, the arrangement of inlets is much like a manifold problem. Safety considerations make removal of stormwater from pavement a critical requirement. Since the barriers are often located very close to the driving lane and no flexibility in size or spacing of the inlets is afforded, it is essential to be able to assess capacity of the system to ensure that water does not spread on to the pavement.

Purpose and goal

The purpose of the investigation reported here was to establish the hydraulic performance of barrier wall inlets, as a first step to evaluating the capacity of the barrier wall drainage system. To accomplish this goal, experimental measurements of the discharge characteristics of various aperture configurations were obtained both under sump and transverse flow conditions. Various full scale configurations for drainage apertures were tested in a tilting flume experimental facility. Both the cross and longitudinal slope of the flume could be varied, with zero longitudinal slope corresponding to sump conditions (no channel velocity). Discharge rates of individual inlets have been measured as a function approach flow rate and pavement slope parameters for supercritical conditions.

Findings and conclusions

This report is divided into two components and several appendices are included. The first part consists of a description of experiments and analysis of results regarding measurements of flow capacities for barrier inlets. This portion of the investigation follows closely a paper that been previously presented[6] by the Principal Investigator. It is also noted that a previous study of barrier wall inlets was conducted by the PI for the FDOT[4]. While this earlier study yielded considerable information, it was desired to continue the experimental work (and develop a practical design aid for applications as discussed below). In these experiments, the capacities of isolated, single inlets were measured under conditions of long approach distances and no runoff. Longitudinal and cross

slopes were varied over ranges covering most field conditions, including sump flow. The principal result of this portion of the study was the development of several empirical correlations describing capacity. Several other conditions of interest were also studied including some measurements of the transition from supercritical to subcritical flow and possible methods for enhancing capacity (this latter investigation was not found to be productive, however). Finally, conclusions reached as a result of this experimental investigation are summarized.

The second part of this investigation discusses the development of a design and planning model intended to aid in the estimation of spread for practical application of inertial attenuators. As part of this effort, a more advanced computational program was first constructed as a preliminary step to understanding how the flow along a wall of attenuators actually develops. Subsequently, this information was used to build a simplified spreadsheet program suitable for general usage. This program (delivered separately to the FDOT) computes flow past barrier walls set on grade and includes the possibility of a sag curve. The program (in spreadsheet format) has the following three components, each occupying a single sheet: a variable slope section with flow from left to right, a variable slope section with flow from right to left, and a section representing the ponded region that will form near a minimum elevation section. An example problem is analyzed using the spreadsheet program. This program can also be utilized to estimate flow on simple slope conditions.

Benefits

The principal benefit of this research is expected to be improved safety at construction sites, obtained by application of the hydraulic capacity relationships developed during this investigation. This application will likely be facilitated by the availability of predictive modeling methods for systems of barrier installations. Reduced accident events are anticipated to result in cost savings on construction projects.

This study was eventually expanded to permit the further development of a second generation predictive modeling program with several advanced features. This program, along with a tutorial manual, has been delivered to the FDOT under separate cover.

(this page intentionally blank)

INTRODUCTION

Temporary concrete barriers (inertial attenuators) are often installed at highway construction sites, on the edge of driving lanes for vehicular safety (Figures 1 and 2). To permit storm water drainage from the traffic lanes, one or more cutouts are included at the bottom of each barrier block to form a small rectangular aperture for drainage when the block is placed on the pavement. Thus a continuous array of barrier blocks along the edge of the pavement forms a configuration similar to a curb and gutter, with closely spaced inlets for drainage. This manifold arrangement shares some common characteristics with channels fitted with side weirs for irrigation [1,2] and because of the range of longitudinal slopes and flow rates, the velocity of the water stream passing the inlet can vary from supercritical to stagnant.

During a rainstorm, pavement drainage results from the accumulation of runoff at the gutter due to the cross slope of the roadway surface (Figure 1). If the pavement also has longitudinal slope this accumulation develops into a shallow flow along the side of the roadway. Curb inlets act as local sinks to remove some of the accumulation from the gutter, but water not removed by an inlet continues on as bypass flow to the next inlet. Depending on the volume of flow in the gutter, water may spread back onto the pavement for some distance to become a hazard to traffic. Because these barriers are often found on construction sites where the shoulder is limited, the possibility of dangerous spread is greater than for established roadways. If the rate of removal at an inlet is not at least equal to the accumulation between inlets, the spread will increase with distance along the gutter. Even after a storm event ceases, flow in the gutter persists for some time from residual drainage.

Conventional pavement drainage systems usually consist of a broad shoulder beyond the driving lanes and an efficient gutter fitted with high capacity inlets. In designing for proper drainage, there is considerable flexibility in the spacing of the inlets to accommodate the maximum projected runoff. In contrast, the drainage system resulting from the placement of inertial attenuators with cutouts on the pavement consists of a large number of openings at closely spaced intervals. Adequate pavement drainage can only be ensured by estimating the runoff, then comparing this quantity with potential system capacity. When barriers are employed, the spacing between the inlet openings is fixed so that there is no opportunity to improve capacity by choice of spacing, as would be the case for a conventional drainage system.

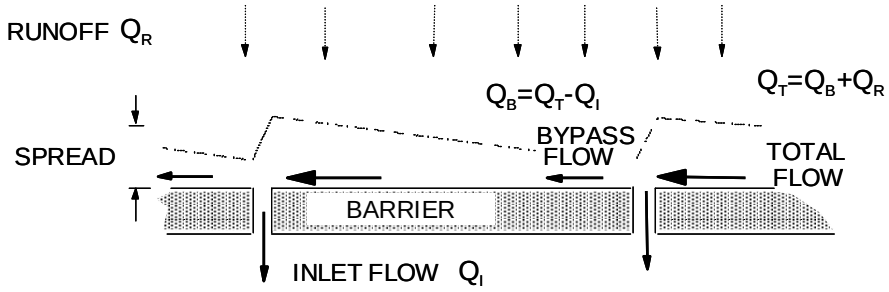

Figure 1: Barrier wall drainage system Top shows typical site installation of a line of inertial attenuators. Note chipping evident at some inlets due to handling. Bottom sketch shows plan view of flow path along barrier wall. Spread is maximum just upstream of inlet entrance.

SINGLE INLET BARRIER

CLOSEUP OF INLET

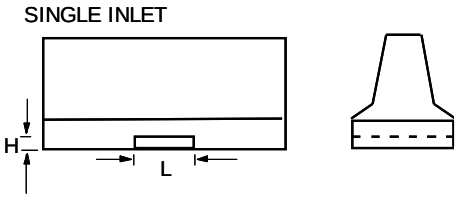

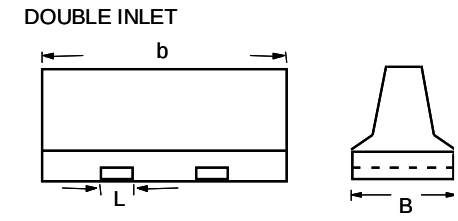

Figure 2: Close-up detail of attenuator and definition sketch for inertial attenuator. Dimensions of a standard single opening barrier (FDOT Index 415[3]); b=11.81 ft, B=2 ft, L=2.58 ft, H=0.167 ft. The two inlet configuration (with L=.5 ft.) is no longer applied to drainage situations in Florida.

The purpose of the present investigation was to improve understanding of the hydraulic performance of drain inlets for inertial attenuators, especially to provide the type of information needed to ensure adequate capacity. Barrier inlets are much smaller than conventional curb inlet configurations and are usually much less efficient. In part, this deficiency is caused by the absence of approach fairing or drop-down at the entrance, as would be found on a conventional inlet. In Florida, only 2.58 ft openings are employed[3], but other states use both smaller and larger sizes. An alternative configuration, including two smaller inlets, previously used in Florida is shown for reference.

As shown in Figure 1, continuity for the flows (Q) at each inlet gives

$$Q_B = Q_T - Q_I \tag{1}$$

where the subscripts T, B, and I refer to total, bypass and inlet respectively. The total flow just upstream of an inlet is the combination of carry over from the previous inlet and the accumulated runoff between inlet stations, Q_R.

$$Q_T = Q_B + Q_R \tag{2}$$

The total flow in the channel may increase or decrease along the roadway depending on how much of the runoff is captured at each inlet. If all runoff accumulated between inlets is captured, a steady state is reached where Q_T is constant just upstream of each inlet. It is likely that under storm conditions, the accumulation due to runoff is much smaller than bypass flow, and that the total flow is much larger than the capacity of any single inlet.

A conventional approach to determining system capacity for roadway drainage is to assume the flow is at normal depth just upstream of the inlet and that the inlet capacity is determined by the approaching flow rate, the inlet configuration and the orientation of the pavement. A line of closely spaced inlets may not behave in the same way as conventional, widely spaced curb inlet configurations however, since the flow may not achieve the characteristics of uniform flow between inlets. Furthermore because of the short spacing interval, it is possible that flow into an inlet cutout may be influenced by large disturbances at the adjacent inlet upstream.

The results of a previous investigation[4] suggested that the capture at a barrier inlet could be directly correlated with depth of flow in the gutter immediately upstream, with pavement slope having little or no influence. Thus, if flow into a barrier inlet is not substantially influenced by disturbances at the inlet immediately upstream and the flow is close to normal depth near the entrance, the evaluation of drainage capacity of the barrier wall system could be considerably simplified. A simple method for design calculations based on these

assumptions was proposed in Reference 4. A direct correlation between inlet flow and upstream depth would permit Equations 1 and 2 to be satisfied since the depth at the inlet could be estimated from Manning's equation, so that the spread into the driving lane could be predicted. One goal of the present investigation is to verify this conjecture and to develop an accurate correlation. Accordingly, a series of experimental measurements of capacity for individual inlets was initiated.

The foregoing discussion applies to flow on grade with supercritical velocity past the face opening of the inlet (referred to here as transverse flow). In contrast, at the base of a long slope as the pavement becomes level, the flow first slows and then transitions to a subcritical condition, resembling the flow down a spillway into a reservoir. At this point, a pond develops. Inlets in the pond area must handle all local runoff plus the accumulated bypass from the adjacent slope. Assuming that the line of inlets continues, stagnant water will then be removed from the pond area by inlets performing like weirs or if filled, as orifices. In this region an increase in spread may occur, as the pond depth increases until the total capacity for drainage matches the net accumulation. Consequently, part of this investigation was to examine the transition to a stagnant condition and to measure the capacity of the drainage inlets in these circumstances.

EXPERIMENTAL FACILITY AND OBSERVATIONAL METHODS

In the investigation reported here, capacity measurements for single inlets were made using full size models (constructed from resin-coated plywood) set in a flume over a large fiberglass reservoir tank. Water was delivered by centrifugal pump to the upper end of the bed via a large vertical riser, turning at the top and discharging into a flow straightener, approximately 26 feet upstream from the inlet. The facility is shown in Figure 3.

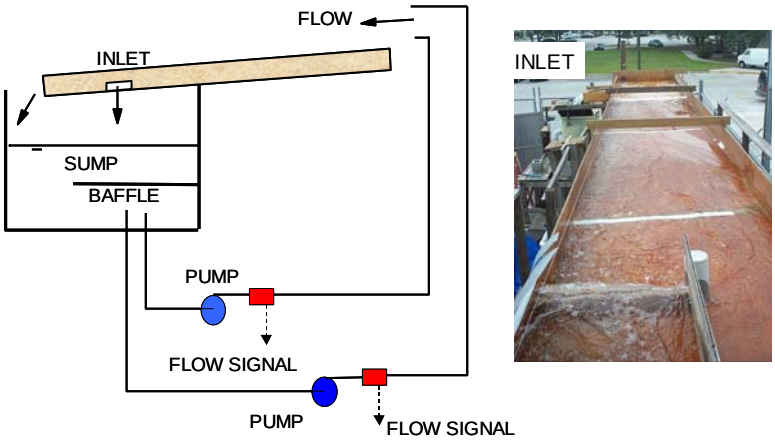

Figure 3: Schematic of experimental facility and photograph of flume.

The flume bed was arranged to tilt at cross slope S_c and longitudinal slope S_o, simulating pavement geometry. These conditions were achieved by jacking and shimming the support of the bed, while checking cross slope with a long level. A line level was utilized to check the longitudinal slope. The sidewall of the flume (representing the vertical edge of the barrier) made a 90° angle with the pavement, forming a triangular section for flow of depth h. The cross slope is small so that the spread is approximately the same as the length across the pavement and the depth h to the vertex of the channel is very close to the measurement y, along the wall to the same point. Thus, the spread is related simply to the cross slope ($T \approx y/S_C$) and comparable relations apply for the area and hydraulic radius. The Froude number for the channel flow may be estimated (based on the average depth of flow),

$$Fr \approx \left(\frac{8}{g}\right)^{1/2} \frac{Q_T S_C}{y^{5/2}} \qquad (3)$$

where g is the acceleration of gravity (a more complete discussion for channel flow relationships is given in Appendix B). Flows in the channel and past the inlet are shown in Figures 4 and 5.

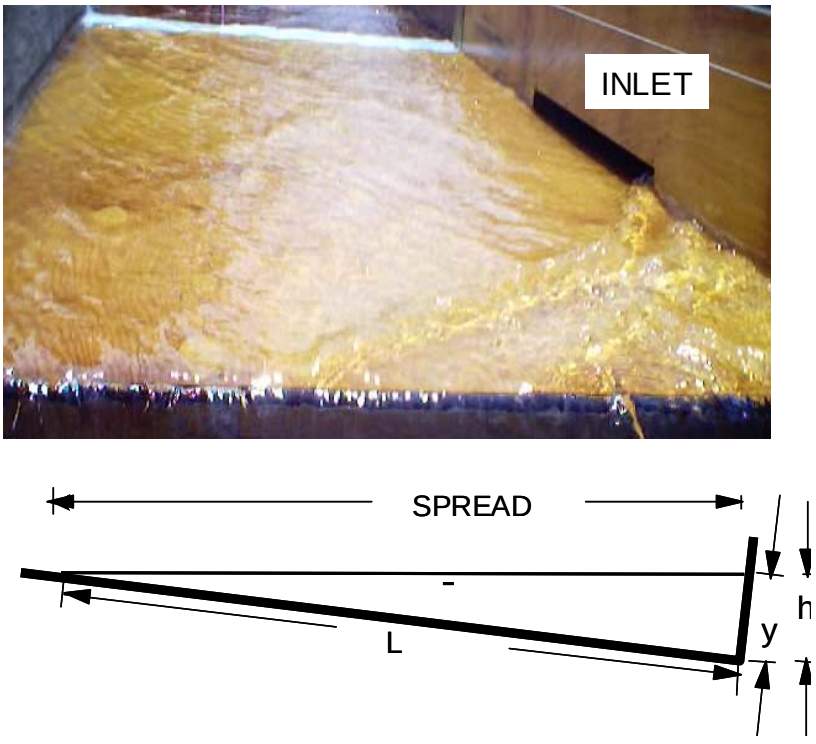

Figure 4: Bed configuration, definition sketch and detail of flow at inlet.

It has been suggested[5] that because the surface width of the flow is very large in comparison to depth, the standard formulation for a channel of triangular cross section is not completely satisfactory for predicting flow conditions and experimental evidence appears to confirm this discrepancy. An alternative formulation (yielding a value about 20% higher) has been developed by integrating Manning's equation for infinitesimal rectangular elements of variable depth across the channel width, giving

$$Q_T \approx [\frac{3kS_0^{1/2}y_n^{8/3}}{8nS_C}] \quad (4)$$

Here k is a dimensional constant depending on the choice of units. (1.49 in English units). Again, the normal depth y_n is measured at the wall. A simple backwater program was developed to provide an estimate of the bed length required for the flow to attain normal depth from the initial point of discharge. Assuming the flow enters the bed at critical velocity, calculations indicate that near uniform flow conditions are attained within the approach length allowed (26 feet) for the conditions investigated here. This estimate does not account for major disturbances such as standing waves in the channel, however.

Discharge onto the bed was measured directly with paddle wheel type sensors (detecting velocity) mounted in the supply lines. Inlet flow was captured by a catch tank and returned to the reservoir through an instrumented discharge or in some cases, diverted to a weigh tank to measure lower flow rates. Water bypassing the inlet was returned to the reservoir through an instrumented line. Accurate measurement of inlet, bypass, and total flow were complicated by the fact that the inlet flow is only a fraction of the total flow, so that relatively small errors in measurement of the total flow might strongly affect attempts to satisfy Equation 1. Each flow meter used during these experiments was either directly calibrated or the calibration provided by the manufacturer calibration was employed. Efforts were made to reduce sensor problems caused by air in the flow lines and also by fittings that cause flow disturbances. Consistency checks and supplemental calibration of the flow meters were conducted by blocking off the channel end so $Q_I = Q_T$. For very low inlet flow rates, discharge was measured both by means of a paddle wheel sensor and using a weigh tank for calibration checks. A similar arrangement was used for discharge measurements at low flow. It is believed that the flow measurements reported here are accurate to 5-10% of flow. Reproducibility checks (including resetting the bed slopes) indicated a maximum scatter of about 15%.

Measurement of the water profile elevation was made (to 0.04 inches) at several stations along the bed and four positions across the bed, using a metal gauge with a sharp pointed end. It is noted that in some instances surface waves may

have affected these results. Elevation of the bed bottom was made in the same manner, yielding a depth of flow at each station across the stream. These depth measurements were then fitted to a linear model by the method of least square error using the position of stations across the channel as independent variable. Thus the predicted slope corresponds to the cross slope of bed, while the intercept is the depth of flow at the wall. Spread was also measured directly, although again this determination was complicated by many small disturbances and was considered to be only a qualitative indicator. Spread was observed to be relatively constant approaching the inlet. Depth measurements taken at several points upstream of the inlet exhibited a slight decrease in depth along the direction of flow indicating that uniform flow may not have been achieved in all cases. As discussed later, measurements of Manning's n obtained with these depth observations are in reasonable agreement with expected values, however.

MEASUREMENT OF INLET CAPACITY

Using the methods outlined above, experiments to measure inlet capture were performed for the following slope ranges: longitudinal slope S_0 = 0, 0.5, 1, 2, 4, 5, 6% and cross slope S_C = 1, 2, 4, 6%. These tests were made for single inlets with an extended upstream reach, no upstream inlet and no runoff flow added to the bed (cf. Figure 5). Typical measurements of hydraulic performance of the barrier wall inlet (capture as a function of approach flow) are presented in Figure 6. Flow rate has been reported as a non-dimensional parameter $Q/(g^{1/2} H^{5/2})$, where H is the height of the inlet (0.167 feet). This choice is not interpreted as a scaling parameter, since the inlet does not usually run full (see appendicies). It was observed that total capture occurs for only a very small range of approach flow and that the efficiency of the inlet was relatively low, as expected.

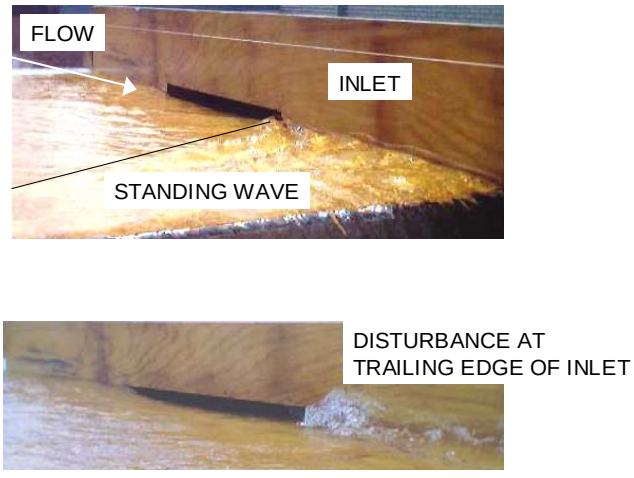

Figure 5: Detail of flow at inlet.

As explained previously, it was of particular interest to examine the correlation between depths in the gutter just upstream of the inlet with the inlet capture. Figure 7 presents the results of this correlation. To develop a correlation using the largest amount of information, a few data sets were included that involved direct measurements of depth at the wall (rather than an extrapolation). Results similar to those of Reference 4 were obtained. No substantial correlation with cross slope or longitudinal slope was found for the ranges examined. This observation indicates water enters the inlet much like a sill flow, probably due to the lack of entrance development.

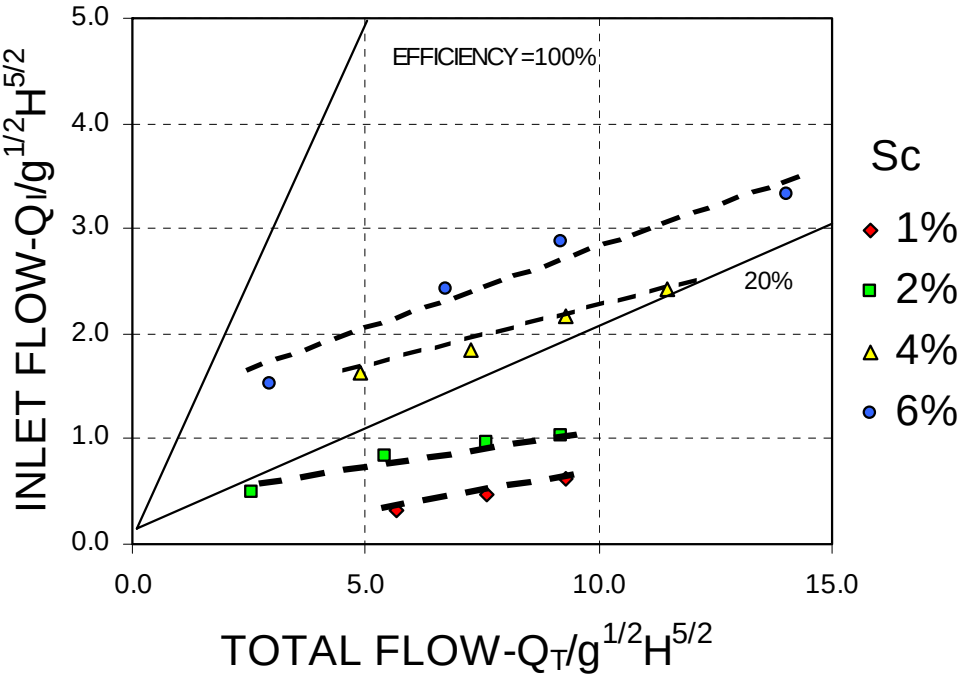

Figure 6: Typical inlet performance, Q_I vs Q_T (nondimensional). Longitudinal slope 1%, cross slope variable. Lines of constant efficiency have been added for reference.

.

.

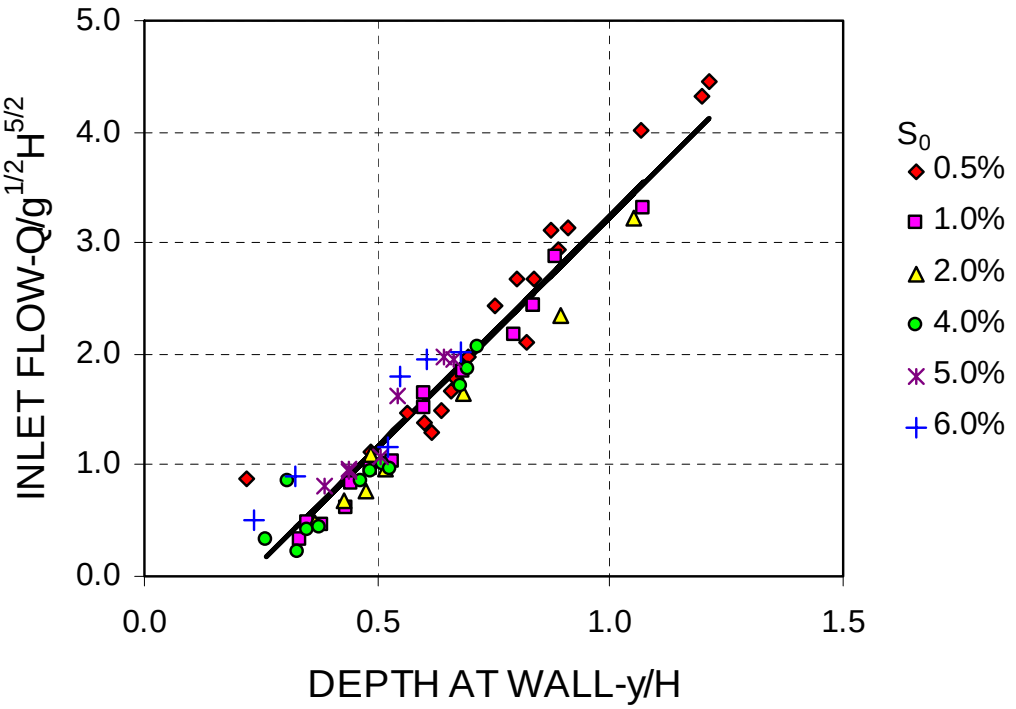

Figure 7: Inlet flow (non-dimensional) vs. wall depth (non-dimensional). Variable longitudinal and cross slope. A linear correlation for transverse flow past the inlet has been added. For simplicity, only the longitudinal slopes has been identified by separate symbols. Note poor performance at small depth.

A correlation between inlet flow and depth just upstream of the inlet has been developed for this data. While the data terminate at the origin, to obtain an economical (but accurate) representation, a simple linear model with intercept was adopted here (Figure 7).

$$\frac{Q_I}{g^{1/2}H^{5/2}} = 4.16\frac{y}{H} - .92 \qquad (5)$$

To apply this correlation, the normal depth immediately upstream of the inlet is calculated for the total flow (assuming that Manning's n and the slope of the pavement is known), then the inlet flow, the spread and the bypass flow can be obtained directly. This procedure can be continued as required along a line of inlets on grade to evaluate system performance. Satisfactory capacity is

indicated by an acceptable spread. Scaling of inlet capacity is discussed in the appendicies.

In many field installations, pond formation at the bottom of a grade is likely to be a more serious concern than spread along the grade, however. The size of the pond that forms is determined in part by the final bypass flow into this area and by the capacity of the inlet when the flow is stagnant. Supplemental experiments to evaluate performance under sump conditions (S_0=0%, variable cross slope) were conducted. These results were found to be comparable with those of Reference 4 and are shown in Figure 8. For the range of depths shown y/H <1.4, so that the flow is within a weir regime and a correlation with a conventional capacity equation is possible.

$$Q = C_{DW} L\sqrt{2g}\, y^{3/2} \tag{6a}$$

A value for C_{DW} of 0.25 provided an optimal fit to the data. It should be noted that the depth parameter for sump flow cannot be interpreted in the same manner as that for the inlet with transverse flow, which is supercritical. Here y is interpreted as the pond depth. Similarly, for orifice flow, a correlation of C_{DO} was obtained for use in

$$Q = C_{DO} LH\sqrt{2g}\, y^{1/2} \tag{6b}$$

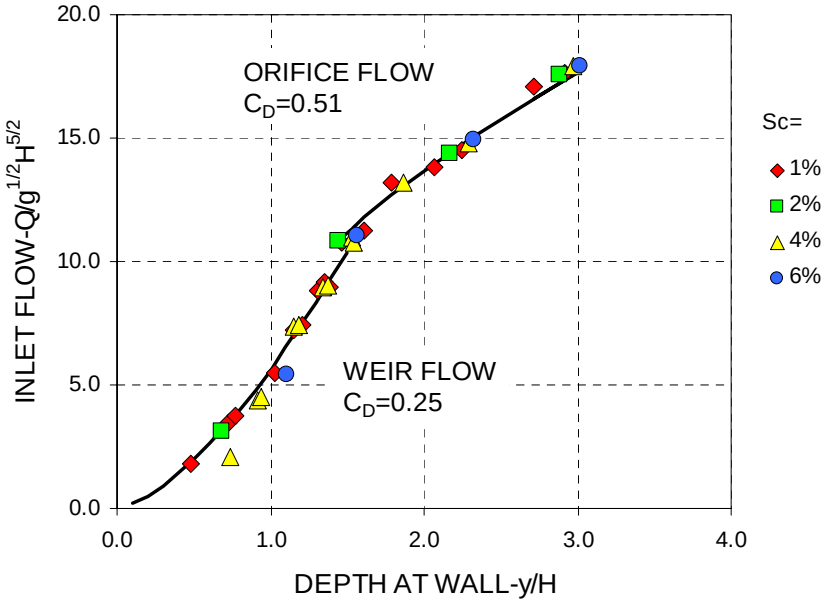

Figure 8: Sump performance for inlet. Both weir and orifice correlations are shown, with transition at y/H≈1.4.

As a check on the consistency of the experimental measurements, the measurements of flow rate and depth were utilized to determine Manning's n for the bed by rearranging Equation 4 assuming normal depth at the measurement station.

$$n \approx \frac{3kS_0^{1/2}y_n^{8/3}}{8Q_T S_C} \tag{7}$$

It is realistic to assume that this quantity remained relatively constant over all experiments, except for normal aging of the surface and imperfections due to maintenance operations. A quality comparison should be possible using measured values for each of the parameters. Manning's n determined in this manner for the same data set shown in Figure 7 yielded a value of n=0.0098. This value is slightly lower than expected but still in reasonable agreement with typical values of n for any relatively smooth surface. In making this estimate, it is recognized that the measurement of depth is not highly accurate, and that this quantity is raised to the 8/3 power (which tends to magnify the effect of measurement error).

OTHER COMPLICATING FACTORS

Several other issues complicate the observations of inlet capacity.

a) Interaction between adjacent inlets: As mentioned previously, a return to a normal depth condition in the interval between inlets is not assured but backwater estimates indicate this is likely, even with the addition of runoff. Not only are the barrier inlets relatively closely spaced but also a standing wave is usually observed trailing from the back edge of the inlet that may influence the performance of the inlet down stream. Experiments intended to clarify the possible interaction between inlets were conducted at half scale. Direct measurements of flows into several inlets are presented in Figure 9. Two important conclusions can be drawn from these observations. Tests conducted with just the downstream inlet open compared to tests with both inlets open were virtually identical (after correction for upstream drawdown), so that interference is not likely to be a large problem. It is noted however that these observations were made under limited conditions and that other slopes and flows may exhibit modest variations.

The second important observation is that the capacities measured for one-half scale are very comparable with full size testing, indicating that direct linear scale up of results is realistic. This assumption is not the same as conventional scaling (Appendix C), corresponding instead to a horizontally distorted model. Conventional scaling appears to be realistic also but only one point could be verified.

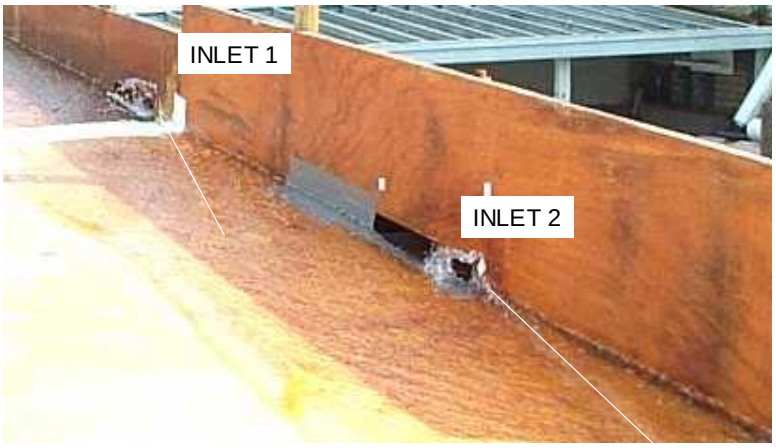

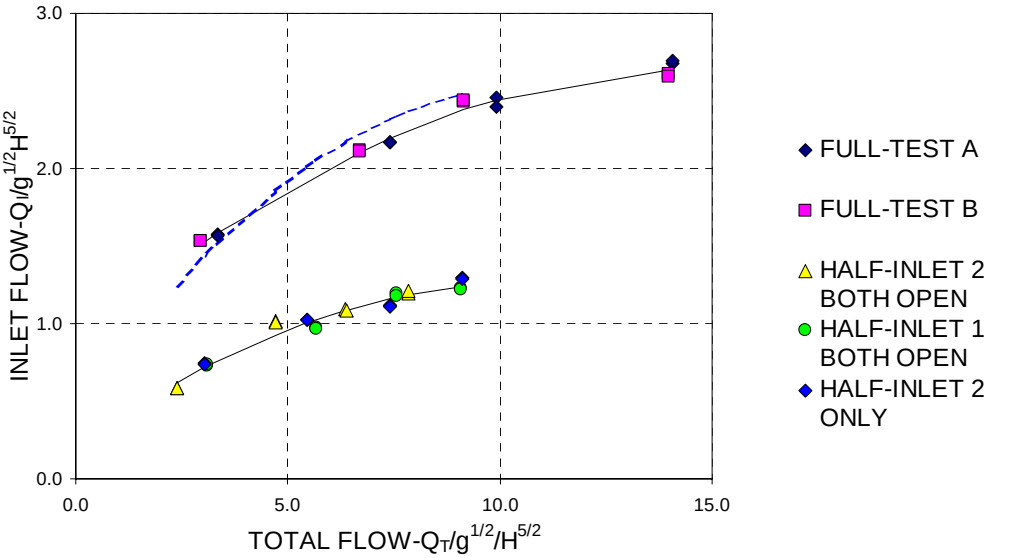

Figure 9: Interaction tests for one flow condition. Photograph above shows flow and wave structure near adjacent inlets. Comparisons of capacity for S_0=0.01 and S_C=0.04. Interference tests conducted at one-half scale and compared to full size tests

b) Flow transitions at the inlet. It is possible to induce a transition flow where the inlet is partially flooded and a hydraulic jump is present in the inlet, as illustrated in Figure 10. Similar conditions have been observed during investigations of side weirs[1,2], and may well be the type of transition that develops from flanking slopes to a pond forming in a depression. It appears that such transitions are most likely to form at inlets because the capacity for inlet flow under stagnant conditions is so much larger compared to that for transverse flow conditions. At present, it appears that no serious implications arise from this flow condition, however a more extensive study may be warranted in the future. A related question concerning the effect of backwater elevation on the inlet capacity was raised but not investigated here.

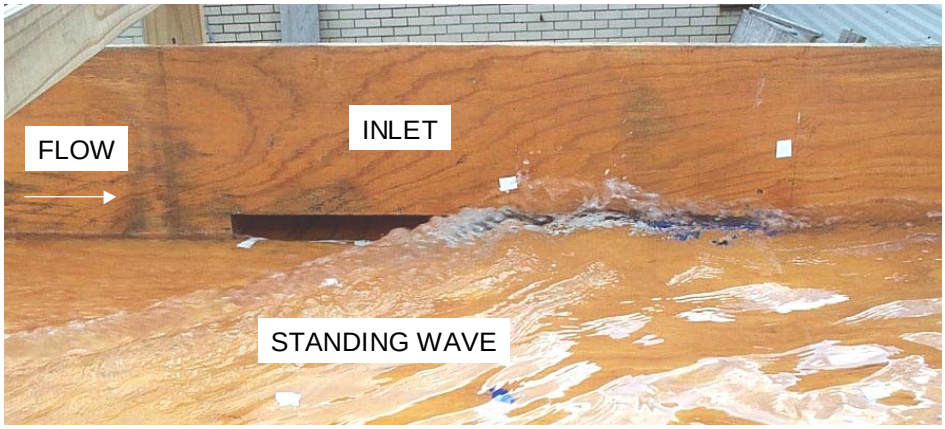

Figure 10: The transition condition arising from a hydraulic jump at the inlet. Note the upward facing standing wave that forms in this case.

c) Modifications for improved flow at the inlet: During the course of this investigation, a series of experiments were conducted to examine several ideas to improve capacity of the inlets. These modifications principally consisted of small blocks placed at various positions in and around the inlets, intended to stimulate depth changes that would translate to capacity increases. In generally these tests were not sufficiently encouraging to continue, and at this time it is recommended that no further efforts be made in this direction.

Several alternative configurations were inspected as possible improvements. Some states use much larger openings (> 4 feet) and the Department is considering a change to a higher and longer aperture split into two closely adjacent parts. The scaling results previously obtained suggest that simple transformations can be utilized to estimate capacity. It is noted in passing that an alternate modification consisting of a change to expand the flow passage through the block, angled along the flow direction was discussed but not tested.

MODEL DEVELOPMENT

Concrete barrier walls are presently utilized both as temporary and permanent installations along roadways and overpasses. Just as in the case of curb and gutter installations, it is extremely important to provide for adequate drainage of roadway runoff accumulating at the side of the pavement. The planning/design task confronting the engineer is to make use of the information developed in the first portion of this report to evaluate the flow along a series of inertial attenuators aligned at the side of the roadway. A principal problem is to account for the multiple openings, runoff flow and variable slope that may include depressed regions where water ponds. The flow resulting from these circumstances may be visualized as follows (Figure 11). At the upper extent of a grade, where the line of barriers begins there may be an initial flow entering into the gutter. It is likely that in many cases that this flow is negligibly small, especially if the initial block is set at the top of a rise. Assuming that a substantial rainfall runoff to the side of the pavement exists, water accumulates in the gutter channel along the barrier line down the slope. For minimal initial flow, it is expected that the depth increases in the channel, since cumulative inlet flow is less initially than the cumulative runoff. At some distance along the line of barriers however, the inlet flow balances with the runoff accumulated between inlets and a type of equilibrium condition develops (note however that the runoff flow is only a fraction of the total flow in the channel at equilibrium). The spread oscillates between a local minimum at the downstream edge of each inlet and then grows somewhat until the next inlet is encountered. However, it should be noted that an initial flow at the top greater than this equilibrium means that the flow depth in the channel decreases until the equilibrium state is reached. If the line of barrier inlets terminates on the slope, some bypass (typically about the quantity of the equilibrium flow) will be freely discharged at the end of the line of barriers on grade.

If the line of barriers does not terminate but instead the slope decreases to zero and increases again as the pavement rises again on the opposite side, a stagnant pond will form. It is possible that the most critical spread could develop in this region, instead of on the adjacent slopes. The depth of the pond (which ultimately determines the spread here) will adjust to a depth consistent with the sum of all flow into the pond region equal to the inlet flow out of this region. Since the flow on grade is expected to be supercritical and the pond is stagnant, a transition (likely first to a subcritical state) between these two conditions may be anticipated.

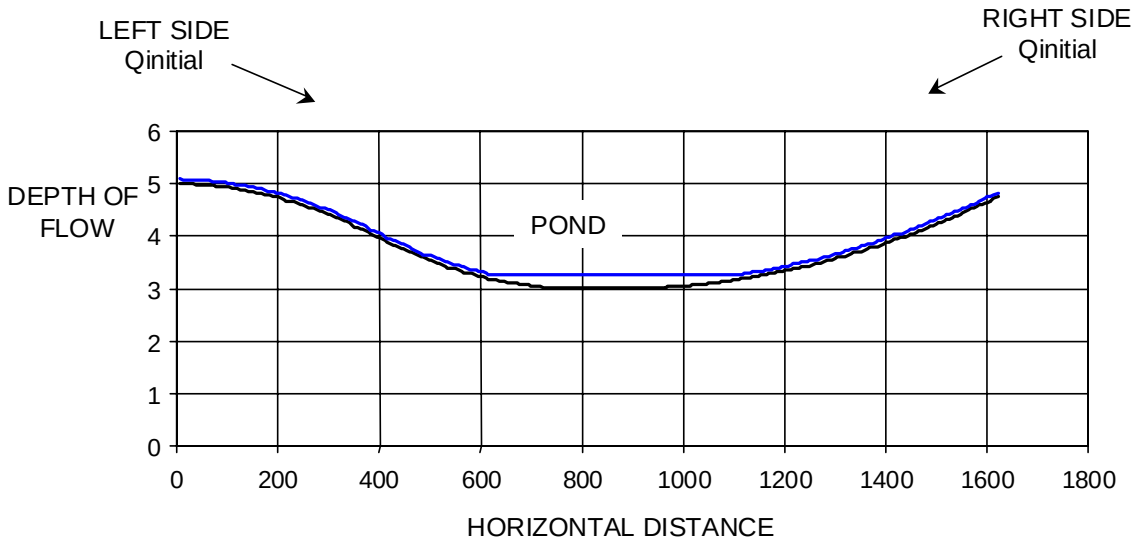

Figure 11: Illustrating a depressed section of roadway resulting in pond formation. For generality, the possibility of initial flow at the top of grade is included.

This remainder of this report is concerned with the development of a modeling program, convenient to use for planning and evaluation purposes. Because of the overall requirement for simplicity, it will be necessary to first examine the consequences of adapting the results of the first portion of this work to modeling. To summarize, empirical relations were developed for the capacity of isolated inlets following long approach distances and without added runoff flow. Likewise relations for sump conditions were also presented. Accordingly, in the discussion that follows, first a detailed model is presented and used to assess various simplifications necessary to develop a second stage, spreadsheet model. This spreadsheet model is then introduced and sample computations are presented.

FLOW RELATIONSHIPS

Consider a line of barrier wall inlets as shown in Figure 12. The segment i includes the region between downstream edges of successive inlets for a distance b along the pavement. The change in elevation between these two points is given by bS_0.

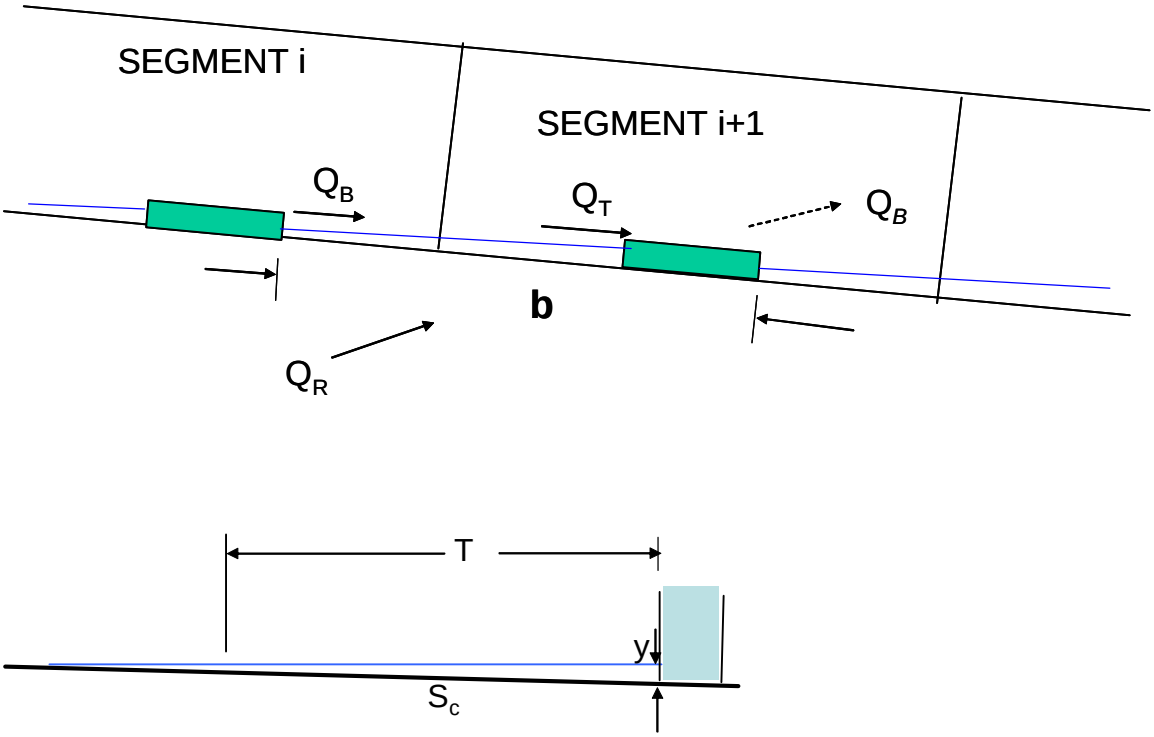

Figure 12: Notation for elevations and flow relationships

Equation 1, representing the flow balance at an inlet i can be rewritten as

$$Q_{Ti} \approx Q_{Ii} + Q_{Bi} \tag{8}$$

Here Q_{Ti} is interpreted as the total flow just upstream of inlet i, Q_{Ii} is the flow into the inlet i, and the bypass flow at the downstream edge is designated Q_{Bi} (inlet efficiency is the ratio of inlet flow to total flow). This relation requires some interpretation due to a small amount of runoff accumulated at the inlet. The total flow can be equated to the runoff accumulated between the upstream edges of successive inlets and the bypass flow from the inlet upstream.

$$Q_{Ti} = Q_{Bi-1} + Q_{Ri} \tag{9}$$

This relation is exact only if the runoff term is interpreted as all runoff accumulated between the downstream edge of inlet i-1 and the downstream edge of inlet i. Runoff can be calculated from the precipitation rate and the pavement area of this segment

$$Q_R = Pwb \tag{10}$$

where w is the width of the pavement and b is the barrier length for single inlet blocks. The empirical relation developed for transverse flow past an inlet entrance on grade will be adopted for this modeling effort

$$Q_I = g^{1/2} H^{5/2} (4.16 \frac{y}{H} - 0.92) \tag{11}$$

This simple linear relation goes to zero at y/H<0.22. Although it is likely that small flow enters the inlet at any depth, the conservative approximation that no inlet flow occurs at less than this cutoff will be made for simplicity. Considering for the moment only cases where bypass exists, the equilibrium spread on grade is found by equating the inlet flow to the runoff and solving for the depth. Thus for constant slope

$$y_e = \frac{H}{4.16} (\frac{Q_R}{g^{1/2} H^{5/2}} + 0.92) \tag{12}$$

so that the equilibrium spread is

$$T_e = \frac{H}{4.16 S_c} (\frac{Q_R}{g^{1/2} H^{5/2}} + 0.92) \tag{13}$$

DETAILED ANALYSIS OF FLOW CONDITIONS ON GRADE

Because runoff is accumulated along the channel, the simple approach to gradually varied flow found in most hydraulic texts is not adequate to describe flow conditions encountered with barrier inlets. An outline of a comprehensive analysis of the flow in the gutter channel including the effect of the runoff flow, following Henderson[7] was introduced in Reference 4. Briefly, assuming that the runoff continuously adds water to the flow in the gutter and that no momentum is added, a differential expression for the gradually varied flow is

$$\frac{dy}{dx} = \frac{S_0 - S_f - \frac{2QdQ}{gA^2dx}}{1 - Fr^2} \qquad (14)$$

A solution technique for this differential equation was developed and implemented in Matlab©. Consider first the case of supercritical flow on a steep slope ($y_c > y_n$). Knowledge of the depth and quantity of flow at the trailing edge of an upstream inlet provides initial conditions to begin the solution, which continues until the entrance to the next inlet is reached. If the computation begins at an upstream point of beginning for the wall with a very small initial flow and depth, the solution process can proceed from inlet to inlet by calculating the depth at the entrance then obtaining the inlet flow from Equation 11 and the bypass flow from Equation 1. A minor simplification was introduced here, in assuming that all the runoff was accumulated between inlets, instead of including that accumulated at the inlet (as discussed in relation to Equations 1 and 2).

To calculate the water depth downstream of the inlet, it is assumed that the specific energy is unchanged across the inlet, yielding the following relationship

$$ay_2^5 - ay_1y_2^4 - Q_1^2\frac{y_2^4}{y_1^4} + Q_2^2 = 0 \qquad (15)$$

where $a=g/2S_C^2$ (note misprint in Ref. 4). As the computations proceed along the slope, the flow along the wall will build until the quasi-equilibrium condition is established as discussed previously.

An example will serve to illustrate this discussion. A line of barriers is placed on a section of pavement having an initial longitudinal slope of 0.02, with a regular decrease in slope of 0.0002 per inlet spacing. The pavement cross slope is 0.02 and Manning's n is 0.016. The rainfall rate is 4 inches per hour and the pavement contributing area is 36 feet wide. A small flow and depth were imposed at the upstream end of the wall, to start the computations (Q_0=0.01 cfs and y_0=0.01 feet). Computations start at the beginning of the wall and continue downstream, with each reach between inlets separately solved using Equation 14. The quasi-equilibrium depth for this case (calculated from Equation 12 is y_e=0.061. The distance along the wall to achieve this condition is approximately 111 ft. Figure 13 shows the progression of solutions between inlets. The changing longitudinal slope eventually forces a critical condition somewhere in the reach near the inlet for barrier number 44, at about 512 feet in this example. After this point is reached, the transition to flow on a mild slope begins.

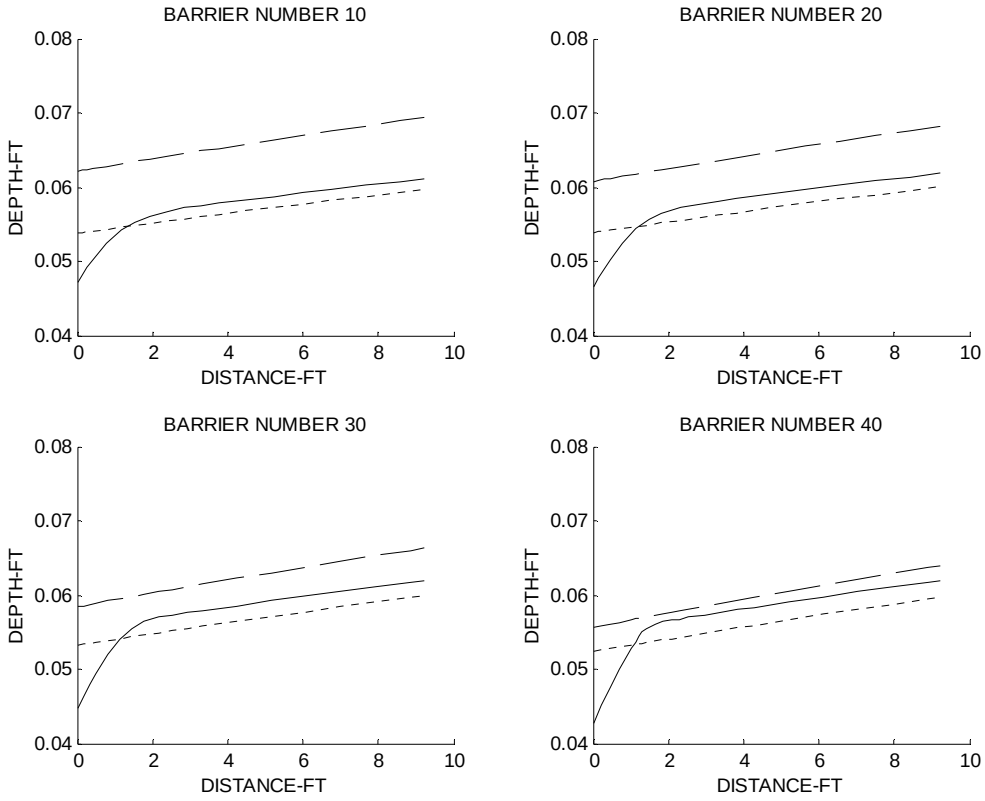

Figure 13: Illustrating the changing flow state between inlets as the slope decreases on grade (supercritical condition). Left side of graph shows conditions immediately downstream of an inlet (at position), the right hand side is the conditions just before an inlet. Barrier length is 11.81 feet and the inlet dimensions are 0.17 feet high by 2.58 feet wide. The flow began on a grade of slope =0.02, with Manning's n=0.16 and rainfall=0.0394 cfs per foot along pavement (4 ips).

The table below shows the state at the end of the reach (just before the next inlet) for each case illustrated in Figure 13.

Table 1: Conditions at inlets as shown in Figure 13. Cross slope 0.02

Inlet	Position	S_0	Y	Yc	Yn	Q	Fr
10	111	0.018	0.061	0.071	0.061	0.136	1.460
20	229	0.016	0.062	0.070	0.062	0.132	1.380
30	347	0.014	0.062	0.069	0.062	0.123	1.280
40	465	0.012	0.062	0.066	0.062	0.114	1.180

For supercritical flow, the depth at the start of each reach (at the downstream edge of an inlet) will be less than normal depth, due to the drawdown caused by inlet discharge. As the flow progresses downstream the depth will increase. In contrast to conventional analysis on gradually varied flow, several numerical experiments such as that shown above indicate that the depth downstream from an inlet rapidly increases to achieve a value somewhat greater than normal depth but less than critical, within a few feet of the upstream inlet (due to the accumulation rate along the reach. After this point is reached the depth of flow lies between critical and normal depth and all depths increase in an approximately linear fashion with about the same slope. Furthermore the assumption of normal depth at the inlet entrance is conservative for supercritical flows as long as the Froude number is greater than about 1.2.

As the slope is reduced, detailed computations over the reach between inlets indicates that the flow depth grows rapidly and may actually achieve critical depth somewhat downstream of the inlet. This behavior was only observed for Froude numbers slightly greater than unity, but before the change to mild slope conditions. Computations became unstable under these conditions and could not be continued. For values of Fr below 1.2, but above 1.0, a better approximation appears to be the average of the critical depth and the normal depth, until these two numbers are equal (Fr=1.0). This condition only persisted for a few inlet intervals before the slope condition changed from steep to mild. For the example above, the onset of a critical condition between inlets was observed to start near inlet number 44 and the transition to mild slope by conventional definition was calculated to occur at inlet number 58, at 678 feet. For reference the minimum elevation occurs at inlet number 101.

Just as in the case of gradually varied flow with no addition, a variety of flow conditions are possible for the case with addition. Depending on flow rate, it can be expected that the approach to a depression will eventually include a region of mild slope ($y_n > y_c$) as an initially steep slope is reduced. Computational modeling indicates the following conditions exist on mild slopes for the example above. The flow at the downstream edge of an inlet will be less than normal depth, and typically less than critical. In this case, the conventional flow classification would be an M3 (supercritical) profile and the depth would increase in the direction of flow, towards critical conditions. Because it is not possible for the flow to remain at critical depth on a mild slope, a switch to an M2 (subcritical) profile is required, since the next inlet will act as a control with flow at critical depth at the entrance.

It is likely that the transition from M3 to M2 profiles will occur through a weak, dispersed hydraulic jump, between the two inlets and extending over some distance along the channel. The exact nature of this transition is unknown and is furthermore complicated by the addition of runoff, and the geometry of the triangular channel. On a mild slope ($y_n > y_c$) , an initially supercritical flow can only

change to a subcritical condition via a local jump condition. Depending on the rate of change of slope this situation may happen repeatedly in the region between inlets for mild slope conditions, until a pond boundary is reached.

The flow approaching the next inlet will be subcritical so that the entrance to the next inlet will be a point of locally critical flow with slight drawdown in the water level just before the inlet, if the inlet is discharging freely Numerical computations of the profile of water depth corresponding to M3 and M2 types (in conventional notation), including the effect of runoff indicate for both cases relatively short reaches are required (cf. Figure 18).

For the alternative (but less likely) case, where the flow at the downstream edge of the inlet is greater than critical depth but less than normal, the flow classification will be an M2 profile (decreasing in direction of flow) since again the next inlet acts a control. In this case the result is the same as the former situation, but no jump is required. The use of Equation 1 to predict discharge for subcritical flow past inlets on grade (assuming critical depth at the upstream edge of the inlet) seems realistic in view of the discussion above.

While the transition region from steep to mild conditions was not examined in full scale experiments, qualitative observations made for a small scale model with multiple inlets indicate that the transition is not abrupt but rather takes place over some distance (including several inlets) in the form of repeated dispersed or extended hydraulic jumps as discussed above.

The following related issues were considered in regard to steep slope flows:

Terminal depth at the inlet

The assumption of normal depth near the end of the reach would be an extremely useful simplification if verified. As shown in Figure 14, it appears that in most cases this assumption is warranted. In the previous figure it can be seen however, that as the slope becomes less steep, normal depth and critical depth become closer (but do not merge as is the case without runoff). When this condition occurs, the flow near the next inlet will be close to critical depth.

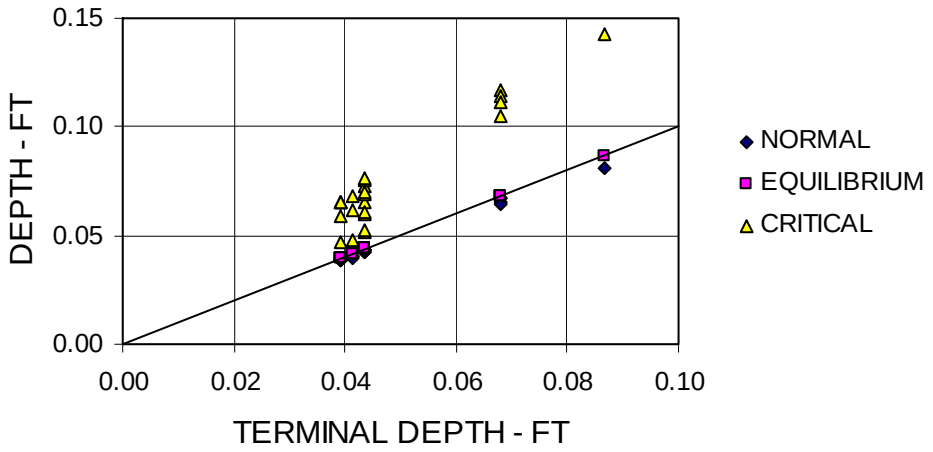

Figure 14: Results of trials conducted for various runoff rates, to examine the equilibrium reached on grade (constant slope). These values were then compared to the critical depth and the normal depth (45° line indicating strong correlation)

Volume of flow in channel on steep grade

Making use of the fact that the equilibrium depth (when attained) is approximately the same as local normal conditions, the approximate volume of flow in the channel can be estimated for equilibrium conditions by assuming that the flow is nearly at normal depth (Figure 15). These values depend on the runoff rate, the bed slope, Manning's n and the cross slope.

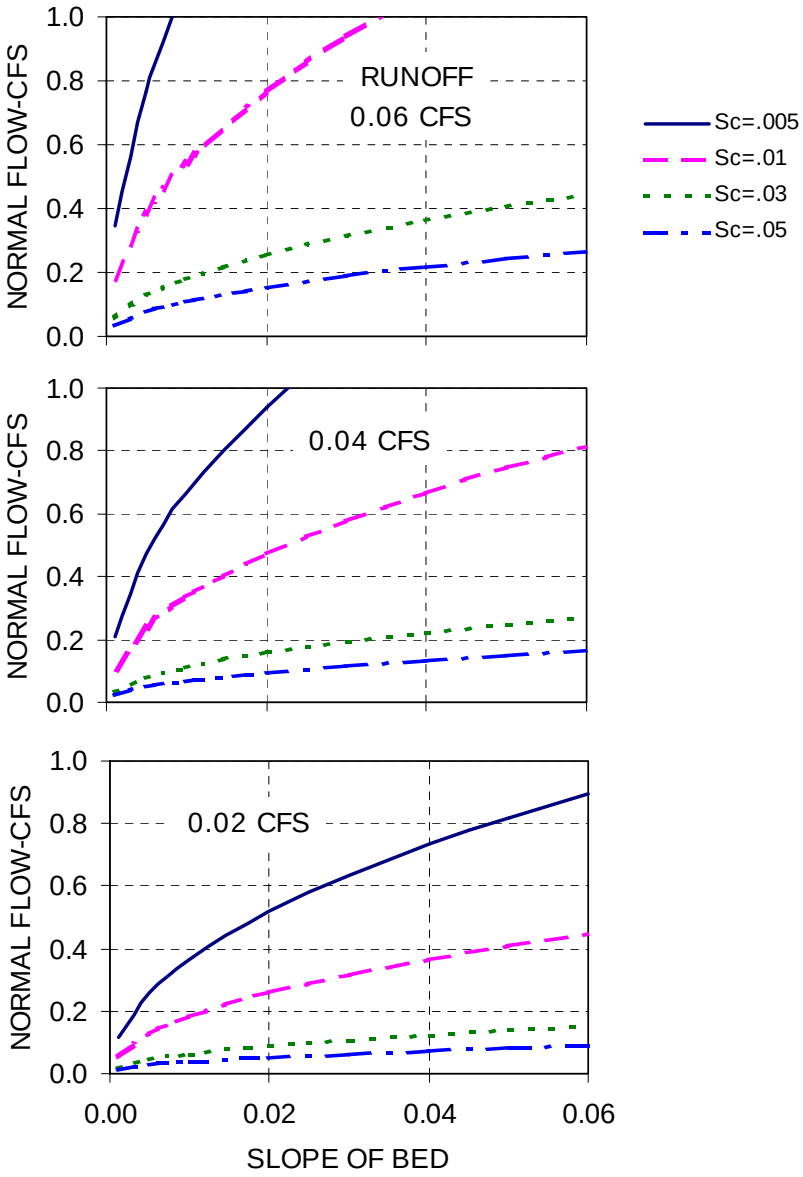

Figure 15: Equilibrium flow rate on grade (maximum between inlets). Manning's n =.01 (correction factor = n/0.01). Calculations based on assumption of normal depth. Runoff rates are per segment.

Spread associated with equilibrium flow can be estimated from the depth, but because this depth depends only slightly on the runoff, spread is primarily a function of cross slope. The spread relationship is shown in Figure 16.

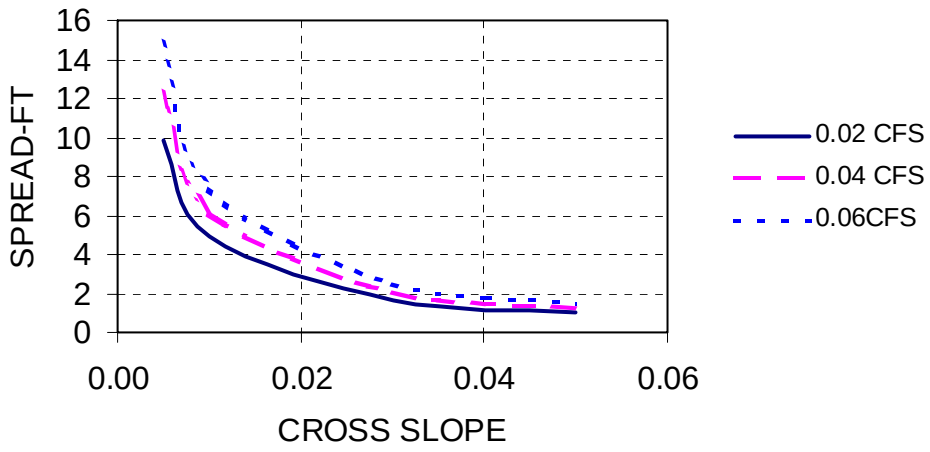

Figure 16: Equilibrium spread on grade as a function of runoff, computed from equilibrium depth and cross slope. Note relative independence from runoff flow rate.

Critical Depth

The critical depth can be estimated from the equilibrium flow rate in the channel, and although this value appears to depend on the cross slope, the normal depth has an inverse relation to cross slope so that critical depth is not actually dependent on this factor (but does depend on runoff). The critical depth is shown in Figure 17.

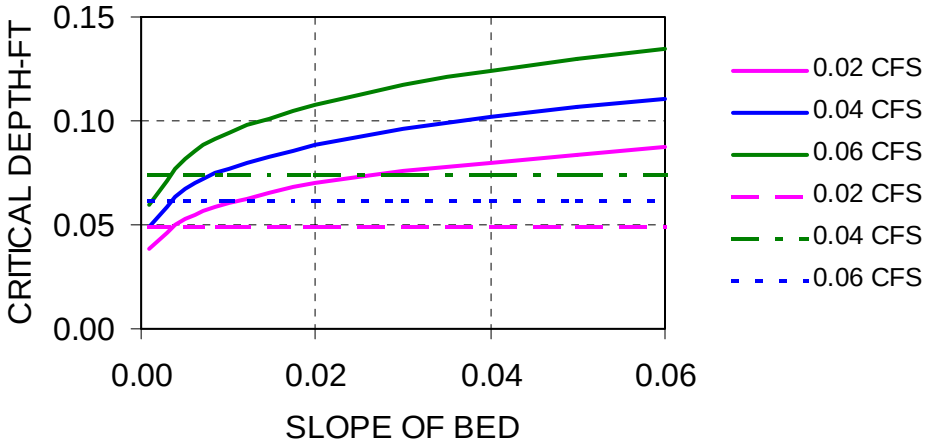

Figure 17: Estimate of critical depth as a function of longitudinal slope from assumption of normal flow at equilibrium depth (critical depth increases with flow rate). The comparable equilibrium flow depths (horizontal lines) for various runoff rates have been added for comparison (quantity increases moving upwards). Mild slope conditions are indicated when the critical depth is less than the equilibrium depth.

As can be seen in this figure, there is a limited range at low slope where the critical depth may be less than the equilibrium depth and the normal depth, indicating a mild slope condition. The situation is much more complex when the flow for a segment begins at supercritical conditions for a mild slope. As in the more elementary textbook situation with no runoff, it appears that the flow approaches critical depth, but must make a transition to a subcritical situation through a hydraulic jump, a transition discussed previously (see Figure 10). This second state then is controlled by a return to critical conditions at the next inlet. Computations indicate that only short reaches are required for gradually varied flow under these conditions. It is likely that because the Froude number is low, the hydraulic jump spreads out for some distance along the reach.

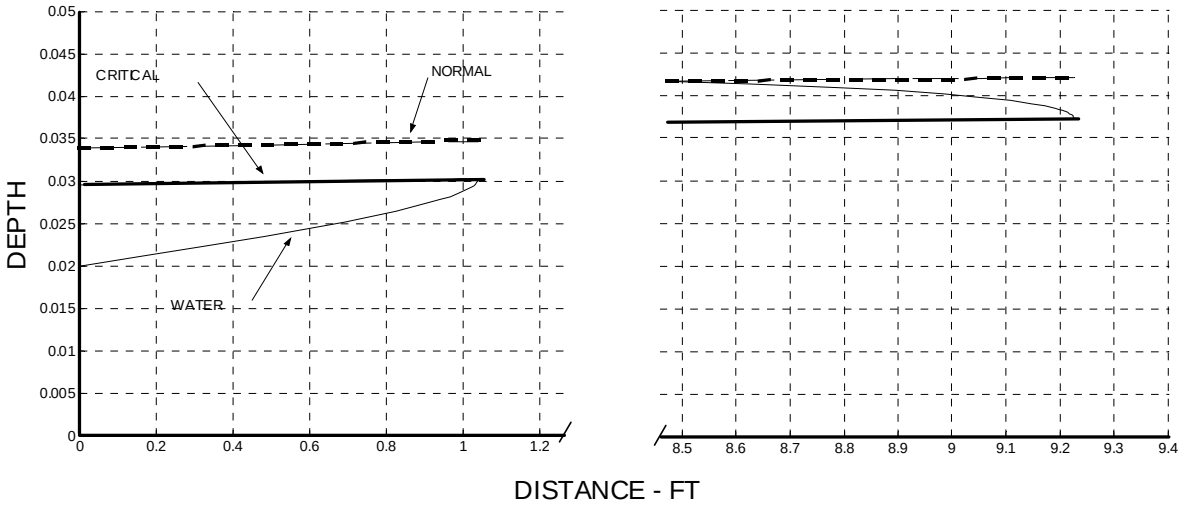

Figure 18: Hypothetical flow profile between inlets on mild slope with a runoff of 0.0074 cfs runoff per segment, longitudinal slope of .002, cross slope .03. Flow starts at left side depth of 0.02 ft. and flow of .01 cfs (arbitrary). At right flow has increased to 0.0174 (computations started at normal depth). It is assumed that these two profiles are joined by a dispersed hydraulic jump starting before the critical depth is reached on the left and terminating at a depth less than normal on right. Example constructed for illustrative purposes only and not intended for application.

Since the flow downstream of the jump is deeper and has slowed, it might be expected that the correlation used to predict inlet flow on steep slopes no longer applies and that the inlet flow is more likely to be of the weir type discharge. Again this condition was not specifically examined but because the capacity of the barrier wall inlets under sump conditions exceeds the capacity under transverse flow by a substantial margin, even if this scenario were true the depth and spread would only be reduced. To be conservative therefore, it seems prudent to assume that the flow is still governed by the transverse flow relationship for all cases except true sump flow.

SPREADSHEET MODEL FOR DESIGN

One task of this research program was to construct and implement a computational model intended to assist in design and planning for drainage of barrier wall inlets. The principal concern here is the ability to predict spread back onto the pavement as a result of accumulation at the wall. While a partial design model was reported in Reference 4, that model lacked the capability to easily

handle sag elevations and resultant ponding. Accordingly, a simplified model was developed and tested, based on the following assumptions and information gained from the results for the detailed model.

1. The assumption of flow slightly greater than normal flow for a simple triangular channel (as discussed previously) will be utilized. About 22% greater flow in the channel is predicted and is therefore conservative.

2. For supercritical flow on steep slopes it will be assumed that the depth of water in the channel returns to local normal depth (as conventionally defined) just upstream of the inlet. For Froude numbers close to unity the critical depth will be used to predict discharge. Detailed modeling indicates that this assumption is conservative.

3. For situations where the slope is decreasing along the flow direction, when the condition of critical flow at the entrance to an inlet is first detected, subcritical flow will be assumed to be the flow state. For subcritical flow on mild slopes the depth of the water at the inlet entrance is assumed to be critical (free flow into inlet).

4. For situations where the longitudinal slope varies, the change will be assumed to be incremental at inlets and the slope will be constant between inlets.

5. For all conditions with transverse flow across the inlet, capacity is assumed to be given by the empirical relation developed in the experimental investigation for both mild and steep slopes (flow rate determined as a function of depth at the upstream edge). Since stagnant conditions result in much higher inlet flow, this assumption appears conservative.

6. To locate possible transitions from flow on grade to a pond (stagnant) condition, the pond depth necessary to produce a flow balance into and out of the pond is calculated. The extent of the pond along the slope can then be determined. The possibility that such a transition might occur right at an inlet is ignored. It is most likely that the flow into the pond is subcritical.

7. For stagnant conditions, inlet flow is evaluated by other empirical relations for orifice and weir flow developed here and elsewhere, based on the local depth in the pond behind the inlet.

Other assumptions and compromises will be introduced and discussed as the spreadsheet model is developed.

WORKSHEETS

Overview

The platform for this program consists of three linked spreadsheets (written in EXCEL©, delivered separately), labeled LEFT, RIGHT, and POND. Both LEFT and RIGHT will treat the flow on grade with variable slope. The POND subprogram will calculate the flow from a ponded region including inlets located on flanking slopes. The first task is to identify the position of the minimum elevation from the information provided on sheet LEFT. The useful information on this sheet does not extend beyond this point, although for generality the program can treat up to 1000 attenuators in each direction. The information provided on RIGHT should mesh with this initial information, with the provision that a horizontal segment between slopes on the left and right are handled independently.

In order to complete the calculations for the pond, an essential step is to determine the depth of water in the pond above the sag elevation, so that the elevation at each inlet in the pond region can be calculated. This step is handled by one of the optimization routines built into EXCEL©. The criterion for this step is that the sum of runoff into the pond area, plus the flow from each side equals the flow though all inlets in the pond region. The flow transition to a stagnant condition occurs at the intersection of the pond level and the water level on the flanking slopes. The possibility that the transition takes place at an inlet is not considered

The program is organized as follows. For the left side, the roadway slopes are supplied from left to right (from the top down). The leftmost point is either the beginning of a barrier wall where the flow is known (possibly zero) or the top of a hill where the flow is zero. The barrier wall extends downwards to the right with a variable longitudinal and cross slope. If the slope decreases along the grade eventually a point of zero slope may be reached. This point may be immediately be followed by a rising slope or a level region (if only a monotonic slope is to be modeled then no further consideration is required).

If a point of minimum elevation is located, then a pond is suspected and the use of the POND sheet will be required. As a final step, the program uses a goal seeking macro to attempt to solve for the depth of the pond (if the slopes at the left and right are separated by a level section, the program data entry treats this region separately, then the flow from the level section is added to the total flow from the pond prior to computations).

Due to the fact that the spread is computed locally, a relatively sharp change in spread will be indicated at the transition to pond. In reality, a gradual transition

will occur as the flow enters the pond. It is unlikely that this simplification would be of concern.

Specific Sheet Content (additional help is summarized in Appendix A, intended to accompany the software)

LEFT - This section includes the downward slope on the left side of the roadway profile. Both the longitudinal slope and the cross slope are locally variable (user input). The maximum length for this sector is set arbitrarily at 12,000 feet (1000 barriers). The elevation must be monotonically decreasing in the direction of flow. Additionally the data entry portion of this section includes a calculation of the runoff flow, (which is assumed to be constant over all three sectors). If a minimum elevation with zero slope (sag) is detected, information regarding this point will be communicated automatically to other sheets. Furthermore, this sheet may be used for calculations of any monotonic slope with or without sag. Such use can be accomplished directly following data entry and computations occur automatically.

RIGHT - This section includes the downward slope on the right side of the minimum. Both the longitudinal slope and the cross slope are locally variable (user input). The maximum length for this sector is set arbitrarily at about 12,000 feet (1000 barriers). The elevation must be monotonically decreasing in the direction of flow. Elevation reference for the right side is independent of the left side but is eventually automatically corrected as discussed further below.

POND - This region is set to include all of the left and right slope regions, but only the inlets submerged by pond water will be used in computations. Provisions are made to include a horizontal section of pavement, with adjacent barriers, or by default this section may simply include a single inlet at minimum elevation. If a horizontal section is included, it is assumed to have the same slope as the last inlet on the adjacent flanking slope to the left and the total number of inlets is taken as the horizontal distance divided by the length of a barrier and rounded. It is possible that the number of inlets could be in error by one but this approximation should not cause serious problems. On command, the operational section of this portion of the program automatically solves for the pond depth, once all data from all three sheets has been entered.

For reference, the definition of spreadsheet columns is given below:

LEFT and RIGHT

COLUMN	DESCRIPTION
A, B	Left blank intentionally to allow user to insert slope change parameters if desired
C	State of flow using modified definitions (see text)
D	Segment - for LEFT and RIGHT, segment number from extreme end
E	So – longitudinal slope for segment. User provided
F	Sc - cross slope for segment. User provided
G	Depth - normal depth of water at inlet start
H	Area - area of triangular gutter section
I	Qrunoff - calculated in data entry section in LEFT
J	Qbypass – flow in gutter immediately downstream of inlet
K	Qtotal – flow in gutter immediately upstream of inlet
L	Qinlet – inlet flow for segment (assuming transverse flow)
M	Spread
N	Distance – total distance to inlet from extreme left position
O	Inlet el - elevation of inlet floor above datum
P	Above sag el – elevation of floor of inlet above floor at sag inlet
Q	Water depth – water depth at inlet based on pond elevation
R	Critical depth based on total flow at upstream edge of ith segment inlet
S	Froude number (same basis)
T	Normal depth (same basis)
U	State of flow (same basis). Used to determine column C

POND

The POND sheet is split into a LEFT and RIGHT side with the segment numbers from the first point of minimum elevation on each side (the extended horizontal section is handled separately). Numbering of segments is from this minimum, corresponding to LEFT or RIGHT numbering. Corresponding columns on the LEFT and RIGHT sheets are reproduced. Columns for weir and orifice flow are both calculated with selection on the basis of depth as explained in the text.

Calculation of pond elevation is made by minimizing the sum of Qright + Qleft + Qrunoff – Qinlet in the pond region. This quantity should be zero. Here Qrunoff is the runoff over the entire pond section and Qinlet is the sum of all inlet flow in the pond region. The spreadsheet incorporates a single action button to accomplish this step automatically. The correct pond elevation is returned. This step is not error trapped however, and if errors occur then probably no realistic solution is possible.

The POND columns are:

C	Offset from sag
D	Segment
E	So
F	Sc
G	Area
H	Spread at inlet
I	Qrunoff for segment
J	Qweir
K	Qorifice
L	Qinlet –choose weir or orifice based on depth in pond
M	Pond spread
N	Distance from initial barrier on left
O	Inlet elevation relative to datum
P	Elevation above sag for inlet
Q	Water depth at inlet
R	INLET FLOW (leaving pond, except horizontal section)
S	RUNOFF FLOW (entering pond, except horizontal section)
T	SLOPE FLOW (flow entering pond from flanking slopes
U	POND NET HORIZ FLOW (runoff–inlet for horizontal section)

Remaining columns reflect the same set for right side.

COMPUTING THE POND DEPTH

Columns R through X of the POND sheet contain the computational results related to pond depth. Once data entry is complete the user is required to click on the "SOLVE" button and the program will pursue an acceptable solution for the depth of the pond (see Figure 19). Details of the solution will appear below. On LEFT and RIGHT segments the regions covered by pond water will be shaded.

SOLVE	**POND FLOW (SHOULD =0)**		**0.0000 CFS**			
	POND WATER EL		**36.00 FT**			
	SPREAD AT SAG		**4.70 FT**			
	WATER DEPTH AT SAG		**0.047 FT**			
	MAX SPREAD LEFT		**5.21 FT**		**Pond index L**	**10**
	MAX SPREAD RIGHT		**5.07 FT**		**Pond index R**	**8**
			POND			
INLET FLOW	**RUNOFF FLOW**	**SLOPE FLOW**	**NET HORIZ FLOW**	**SLOPE FLOW**	**RUNOFF FLOW**	**INLET FLOW**

Figure 19: An example of the solution portion of POND sheet.

INSTRUCTIONS FOR DATA ENTRY (ENGLISH UNITS)

Data entry is normally expected in cells shaded yellow only. Changing values in other areas is possible but may have unintended consequences. With the exception of the slope settings, all entries are made at the top of LEFT, RIGHT and POND

1. Enter Manning's n (default value = 0.01)
2. Enter Initial flow at top of LEFT and RIGHT (default =0)
3. Datum is arbitrary. It is desirable that this value makes sag elevation positive
4. Initial Elevation is that of end of first barrier on LEFT or RIGHT
5. Precipitation rate (inches/hr) is taken as constant everywhere (on LEFT)
6. Enter width of pavement (on LEFT)
7. Enter length of any horizontal section or 0 if none (on POND)
8. Entering slope: the slopes S_0 and S_C at each segment must be provided (on LEFT and RIGHT, not on POND)

Several methods can be used to provide slope data at each inlet entrance. For example, direct entry is possible or data can be taken from a file. A formula to generate the change of slope could be used. Finally, data could be obtained from a vertical curve design program (illustrated in the example below).

EXAMPLE CALCULATION

To illustrate the modeling procedure discussed here, the following example has been analyzed. Inertial attenuators are to be installed along a length of roadway that includes a depressed area flanked by two sloped sections, and planning requires an estimate of the maximum spread of water that might occur during a possible 4 inch/hour storm event. Various portions of the spreadsheet discussed below are shown on the following pages.

Data entry begins on page “LEFT”. Values requiring immediate attention are shaded for convenient identification. For this example, n=.016, and no initial flow is expected at the first inlet. The precipitation rate (specification) has been entered along with the pavement width of 24 ft (assumed constant for the entire extent of the problem).

The longitudinal and cross slope of the left side must be entered. This step can be accomplished by any conventional spreadsheet method, including direct manual entry or file import. In this example calculation, a vertical curve design program was used to generate the longitudinal slope data. Cross slope was held constant at 0.01. Elevations were taken directly from this design program.

No further data entry is required for page “RIGHT” (except for the possibility of cross slope change or initial flow). Here again it is assumed that no initial flow exists at the start of the barrier installation. The elevation for this point is also computed as part of the vertical curve design sheet.

Computations are completed on page “POND”. The final step is to calculate the pond elevation consistent with a flow balance to the pond region. This step can be calculated by clicking on the “SOLVE” button on the POND page. If a satisfactory elevation can be calculated, the extent of the pond will be determined and appropriate segments will be colored blue on the LEFT and RIGHT sheets. The values of the pond depth are constrained to be greater than the elevation of the minimum. It may be true that no solution can be found, most likely indicating a dry pond.

The information on the POND sheet (boxed cells) indicates where the maximum spread will be found. For the case specified here, the pond depth is 0.061 feet, with the maximum spread occurring on the left side above the pond formation 5.4 feet and on the right 5.3 feet. The spread at the pond (6.11 ft) is greater than that on either slope. This conclusion might be reversed under other conditions, however. It is also noted that the pond spread encountered with the older style blocks provisioned with two small inlets (no longer recommended for this application) can develop large spread in the pond region. The solution section has the following appearance:

POND-SOLUTION SECTION

SOLVE	POND FLOW (SHOULD =0)	0.0000 CFS		
	POND WATER EL	11.12 FT		
	SPREAD AT SAG	6.11 FT		
	WATER DEPTH AT SAG	0.061 FT		
	MAX SPREAD LEFT	5.43 FT	Pond index L	4
	MAX SPREAD RIGHT	5.32 FT	Pond index R	3

INLET FLOW	RUNOFF FLOW	SLOPE FLOW	POND NET HORIZ FLOW	SLOPE FLOW	RUNOFF FLOW	INLET FLOW
0.078	0.026		0.0000		0.026	0.078
0.078	0.026				0.026	0.063
0.063	0.026				0.026	0.036
0.036	0.026				0.026	0.007
0.006	0.026			0.1046		
		0.1052				

Figure 20: Solution portion of POND for example discussed.

The corresponding views of LEFT, RIGHT and the remaining areas of POND are shown below.

ENGLISH UNITS

Manning's	n=	0.016							
Inlet height	H=	0.17 FT	Initial flow	Q0=	0.000 CFS	Pond el	11.12 FT	Horiz length	
Inlet width	L=	2.58 FT	Initial depth	Y0=	0.000 FT	Left sag el	11.05 FT	Horiz inlets	
Inlet space	b=	11.81 FT	Runoff flow	Qrunoff=	0.0262 CFS	L sag index	31	Precip rate	
Gravity	g=	32.2 FT/SEC^2	DATUM		0 FT	Dist to sag	361.50 FT	Pave width	
Constant	k=	1.49	Initial el	LEFT EL0=	13.76 FT	Max spread	5.43 FT	Equi depth	

LEFT SLOPE **LEFT SLOPE** **FLOW IS LEFT TO RIGHT**

State of flow	Segment	So	Sc	Depth	Flow area	Qrunoff	Qbypass	Qtotal	Qinlet	Spread	Distance	Inlet el
MILD	1	0.010	0.010	0.023	0.026	0.016	0.000	0.016	0.000	2.29	7.20	13.69
MILD	2	0.010	0.010	0.034	0.057	0.026	0.016	0.042	0.000	3.38	19.01	13.57
CRITICAL	3	0.010	0.010	0.041	0.084	0.026	0.042	0.068	0.007	4.10	30.82	13.45
STEEP	4	0.010	0.010	0.045	0.100	0.026	0.062	0.088	0.013	4.47	42.63	13.33
STEEP	5	0.010	0.010	0.047	0.111	0.026	0.075	0.102	0.017	4.72	54.44	13.22
STEEP	6	0.010	0.010	0.049	0.119	0.026	0.085	0.111	0.019	4.88	66.25	13.10
STEEP	7	0.010	0.010	0.050	0.125	0.026	0.092	0.118	0.021	5.00	78.06	12.98
STEEP	8	0.010	0.010	0.051	0.129	0.026	0.097	0.123	0.022	5.08	89.87	12.86
STEEP	9	0.010	0.010	0.051	0.132	0.026	0.101	0.127	0.023	5.14	101.68	12.74
STEEP	10	0.010	0.010	0.052	0.134	0.026	0.104	0.130	0.024	5.18	113.49	12.63
STEEP	11	0.010	0.010	0.052	0.136	0.026	0.106	0.132	0.025	5.21	125.30	12.51
STEEP	12	0.010	0.010	0.052	0.137	0.026	0.108	0.134	0.025	5.24	137.11	12.39
STEEP	13	0.010	0.010	0.053	0.138	0.026	0.109	0.135	0.025	5.26	148.92	12.27
STEEP	14	0.010	0.010	0.053	0.139	0.026	0.110	0.136	0.025	5.27	160.73	12.15
STEEP	15	0.010	0.010	0.053	0.139	0.026	0.111	0.137	0.026	5.28	172.54	12.03
STEEP	16	0.010	0.010	0.053	0.140	0.026	0.111	0.138	0.026	5.29	184.35	11.92
STEEP	17	0.010	0.010	0.053	0.142	0.026	0.112	0.138	0.026	5.32	196.16	11.80
CRITICAL	18	0.009	0.010	0.054	0.148	0.026	0.112	0.138	0.028	5.43	207.97	11.69
MILD	19	0.008	0.010	0.054	0.146	0.026	0.110	0.136	0.028	5.40	219.78	11.60
MILD	20	0.008	0.010	0.054	0.145	0.026	0.109	0.135	0.027	5.38	231.59	11.51
MILD	21	0.007	0.010	0.054	0.144	0.026	0.108	0.134	0.027	5.37	243.40	11.42
MILD	22	0.006	0.010	0.054	0.143	0.026	0.107	0.133	0.027	5.35	255.21	11.35
MILD	23	0.006	0.010	0.053	0.143	0.026	0.106	0.132	0.027	5.34	267.02	11.28
MILD	24	0.005	0.010	0.053	0.142	0.026	0.106	0.132	0.027	5.34	278.83	11.23
MILD	25	0.004	0.010	0.053	0.142	0.026	0.105	0.132	0.026	5.33	290.64	11.18
MILD	26	0.003	0.010	0.053	0.142	0.026	0.105	0.131	0.026	5.33	302.45	11.14
MILD	27	0.003	0.010	0.053	0.142	0.026	0.105	0.131	0.026	5.33	314.26	11.10
MILD	28	0.002	0.010	0.053	0.142	0.026	0.105	0.131	0.026	5.32	326.07	11.08
MILD	29	0.001	0.010	0.053	0.142	0.026	0.105	0.131	0.026	5.32	337.88	11.06
MILD	30	0.001	0.010	0.053	0.142	0.026	0.105	0.131	0.026	5.32	349.69	11.05
MILD	31	0.000	0.010	0.053	0.142	0.026	0.105	0.131	0.026	5.32	361.50	11.05

Figure 21a: Output on left slope for example discussed.

ENGLISH UNITS

Manning's	n=	0.016	FT								
Inlet height	H=	0.17	FT	**Initial flow**	**Q0=**	**0.000**	**CFS**	Left pond el	11.12	FT	Horiz length
Inlet width	L=	2.58	FT	Initial depth	Y0=	0.000	FT	Right sag el	11.02	FT	Horiz inlets
Inlet space	b=	11.81	FT/SEC^2	Runoff flow	Qrunoff=	0.026	CFS	R sag segment	86		Precip rate
Gravity	g=	32.2		DATUM		0	FT	Dist to sag	1011.05	FT	Pave width
Constant	k=	1.49		Initial el	RIGHT EL0=	14.57	FT	Max spread	5.32	FT	Equi depth
				Initial el wrt L		14.60	FT	Diff sag el R-L	-0.03	FT	

RIGHT SLOPE **RIGHT SLOPE** **FLOW IS RIGHT TO LEFT**

State of flow	Segment	So	Sc	Depth	Flow area	Qrunoff	Qbypass	Qtotal	Qinlet	Spread	Distance	RIGHT Inlet el
MILD	1	0.0036	0.010	0.023	0.026	0.016	0.000	0.016	0.000	2.29	7.20	14.54
MILD	2	0.0036	0.010	0.034	0.057	0.026	0.016	0.042	0.000	3.38	19.01	14.50
MILD	3	0.0036	0.010	0.041	0.084	0.026	0.042	0.068	0.007	4.10	30.82	14.46
MILD	4	0.0036	0.010	0.045	0.103	0.026	0.062	0.088	0.014	4.54	42.63	14.42
MILD	5	0.0036	0.010	0.048	0.115	0.026	0.074	0.101	0.018	4.79	54.44	14.37
MILD	6	0.0036	0.010	0.049	0.122	0.026	0.083	0.109	0.020	4.94	66.25	14.33
MILD	7	0.0036	0.010	0.051	0.128	0.026	0.089	0.115	0.022	5.05	78.06	14.29
MILD	8	0.0036	0.010	0.051	0.131	0.026	0.093	0.119	0.023	5.13	89.87	14.25
MILD	9	0.0036	0.010	0.052	0.134	0.026	0.096	0.122	0.024	5.18	101.68	14.20
MILD	10	0.0036	0.010	0.052	0.136	0.026	0.098	0.125	0.025	5.22	113.49	14.16
MILD	11	0.0036	0.010	0.052	0.137	0.026	0.100	0.126	0.025	5.24	125.30	14.12
MILD	12	0.0036	0.010	0.053	0.139	0.026	0.101	0.128	0.025	5.26	137.11	14.08
MILD	13	0.0036	0.010	0.053	0.139	0.026	0.102	0.128	0.026	5.28	148.92	14.03
MILD	14	0.0036	0.010	0.053	0.140	0.026	0.103	0.129	0.026	5.29	160.73	13.99
MILD	15	0.0036	0.010	0.053	0.140	0.026	0.103	0.129	0.026	5.30	172.54	13.95
MILD	16	0.0036	0.010	0.053	0.141	0.026	0.104	0.130	0.026	5.30	184.35	13.91
MILD	17	0.0036	0.010	0.053	0.141	0.026	0.104	0.130	0.026	5.31	196.16	13.86
MILD	18	0.0036	0.010	0.053	0.141	0.026	0.104	0.130	0.026	5.31	207.97	13.82
MILD	19	0.0036	0.010	0.053	0.141	0.026	0.104	0.130	0.026	5.31	219.78	13.78
MILD	20	0.0036	0.010	0.053	0.141	0.026	0.104	0.131	0.026	5.31	231.59	13.74
MILD	21	0.0036	0.010	0.053	0.141	0.026	0.104	0.131	0.026	5.31	243.40	13.69
MILD	22	0.0036	0.010	0.053	0.141	0.026	0.104	0.131	0.026	5.32	255.21	13.65
MILD	23	0.0036	0.010	0.053	0.141	0.026	0.104	0.131	0.026	5.32	267.02	13.61
MILD	24	0.0036	0.010	0.053	0.141	0.026	0.104	0.131	0.026	5.32	278.83	13.57
MILD	25	0.0036	0.010	0.053	0.141	0.026	0.105	0.131	0.026	5.32	290.64	13.52
MILD	26	0.0036	0.010	0.053	0.141	0.026	0.105	0.131	0.026	5.32	302.45	13.48
MILD	27	0.0036	0.010	0.053	0.141	0.026	0.105	0.131	0.026	5.32	314.26	13.44
MILD	28	0.0036	0.010	0.053	0.141	0.026	0.105	0.131	0.026	5.32	326.07	13.40
MILD	29	0.0036	0.010	0.053	0.141	0.026	0.105	0.131	0.026	5.32	337.88	13.35
MILD	30	0.0036	0.010	0.053	0.141	0.026	0.105	0.131	0.026	5.32	349.69	13.31
MILD	31	0.0036	0.010	0.053	0.141	0.026	0.105	0.131	0.026	5.32	361.50	13.27
MILD	32	0.0036	0.010	0.053	0.141	0.026	0.105	0.131	0.026	5.32	373.31	13.23
MILD	33	0.0036	0.010	0.053	0.141	0.026	0.105	0.131	0.026	5.32	385.12	13.18
MILD	34	0.0036	0.010	0.053	0.141	0.026	0.105	0.131	0.026	5.32	396.93	13.14
MILD	35	0.0036	0.010	0.053	0.141	0.026	0.105	0.131	0.026	5.32	408.74	13.10
MILD	36	0.0036	0.010	0.053	0.141	0.026	0.105	0.131	0.026	5.32	420.55	13.06
MILD	37	0.0036	0.010	0.053	0.141	0.026	0.105	0.131	0.026	5.32	432.36	13.01
MILD	38	0.0036	0.010	0.053	0.141	0.026	0.105	0.131	0.026	5.32	444.17	12.97
MILD	39	0.0036	0.010	0.053	0.141	0.026	0.105	0.131	0.026	5.32	455.98	12.93
MILD	40	0.0036	0.010	0.053	0.141	0.026	0.105	0.131	0.026	5.32	467.79	12.89
MILD	41	0.0036	0.010	0.053	0.141	0.026	0.105	0.131	0.026	5.32	479.60	12.84
MILD	42	0.0036	0.010	0.053	0.141	0.026	0.105	0.131	0.026	5.32	491.41	12.80
MILD	43	0.0036	0.010	0.053	0.141	0.026	0.105	0.131	0.026	5.32	503.22	12.76
MILD	44	0.0036	0.010	0.053	0.141	0.026	0.105	0.131	0.026	5.32	515.03	12.72
MILD	45	0.0036	0.010	0.053	0.141	0.026	0.105	0.131	0.026	5.32	526.84	12.67
MILD	46	0.0036	0.010	0.053	0.141	0.026	0.105	0.131	0.026	5.32	538.65	12.63
MILD	47	0.0036	0.010	0.053	0.141	0.026	0.105	0.131	0.026	5.32	550.46	12.59
MILD	48	0.0036	0.010	0.053	0.141	0.026	0.105	0.131	0.026	5.32	562.27	12.55
MILD	49	0.0036	0.010	0.053	0.141	0.026	0.105	0.131	0.026	5.32	574.08	12.50
MILD	50	0.0036	0.010	0.053	0.141	0.026	0.105	0.131	0.026	5.32	585.89	12.46
MILD	51	0.0036	0.010	0.053	0.141	0.026	0.105	0.131	0.026	5.32	597.70	12.42
MILD	52	0.0036	0.010	0.053	0.141	0.026	0.105	0.131	0.026	5.32	609.51	12.38
MILD	53	0.0036	0.010	0.053	0.141	0.026	0.105	0.131	0.026	5.32	621.32	12.33
MILD	54	0.0036	0.010	0.053	0.141	0.026	0.105	0.131	0.026	5.32	633.13	12.29
MILD	55	0.0036	0.010	0.053	0.141	0.026	0.105	0.131	0.026	5.32	644.94	12.25
MILD	56	0.0036	0.010	0.053	0.141	0.026	0.105	0.131	0.026	5.32	656.75	12.21
MILD	57	0.0036	0.010	0.053	0.141	0.026	0.105	0.131	0.026	5.32	668.56	12.16
MILD	58	0.0036	0.010	0.053	0.141	0.026	0.105	0.131	0.026	5.32	680.37	12.12
MILD	59	0.0036	0.010	0.053	0.141	0.026	0.105	0.131	0.026	5.32	692.18	12.08
MILD	60	0.0036	0.010	0.053	0.141	0.026	0.105	0.131	0.026	5.32	703.99	12.03
MILD	61	0.0036	0.010	0.053	0.141	0.026	0.105	0.131	0.026	5.32	715.80	11.99

Figure 21b: Output on right slope for example discussed. Solution is shown up to inlet 61 only for illustration.

For comparison, suppose the circumstances were changed so that the pavement was 12 feet wide. The results change as shown in Figure 22. Note that now the maximum spread is on the flanking slopes and not at the pond.

POND-SOLUTION SECTION

SOLVE	**POND FLOW (SHOULD =0)**	**0.0000 CFS**			
	POND WATER EL	**94.12 FT**			
	SPREAD AT SAG	**3.96 FT**			
	WATER DEPTH AT SAG	**0.040 FT**			
	MAX SPREAD LEFT	**4.77 FT**		**Pond index L**	**8**
	MAX SPREAD RIGHT	**4.71 FT**		**Pond index R**	**6**

INLET FLOW	**RUNOFF FLOW**	**SLOPE FLOW**	**POND NET HORIZ FLOW**	**SLOPE FLOW**	**RUNOFF FLOW**	**INLET FLOW**
0.041	0.016		0.0000		0.016	0.041
0.041	0.016				0.016	0.041
0.039	0.016				0.016	0.037
0.036	0.016				0.016	0.030
0.030	0.016				0.016	0.021
0.024	0.016				0.016	0.011
0.017	0.016				0.016	0.001
0.009	0.016			0.0800		
0.003	0.016					
		0.0800				

Figure 22: Alternate circumstances (for example presented) resulting in maximum spread on flanking slopes.

COMPARISONS BETWEEN DETAILED PROGRAM AND SPREADSHEET

Several comparative tests were made for the computational model and the spreadsheet. First, the approach to equilibrium was calculated by both methods assuming a constant slope for various initial conditions. The results are shown in Figure 23. In this case the depth just upstream of the inlet was found to be slightly higher than normal depth; hence a slightly higher inlet flow results in comparison to the spreadsheet model. It appears that this result may be caused by the slight correction for uniform flow noted previously. In any case the variation is not large and it is concluded that the spreadsheet model is sufficiently accurate for design and evaluation.

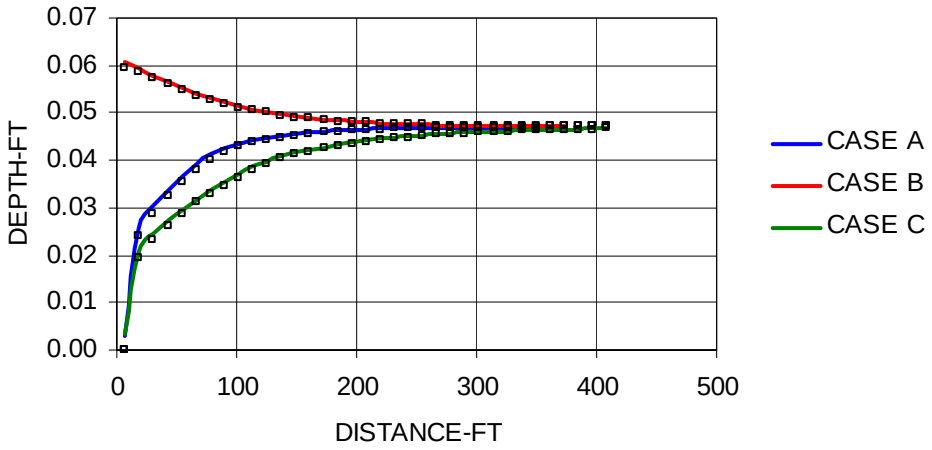

Figure 23. Depth variation on constant slope, comparison between spreadsheet model (symbols) and detailed solution (solid line). Case A: S_0=0.01, S_C=0.01, Q_{init} = 0.0, 95% equilibration length= 124 ft. Case B: S_0=0.01, S_C=0.01, Q_{init} = 0.3, 95% equilibration length=142 ft. Case C: S_0=0.03, S_C=0.01, Q_{init} = 0.0, 95% equilibration length=228 ft. For all cases n=0.01 and runoff equivalent to a 6 inch/hr storm (pavement width =10 ft). Final depth for all cases =0.047 ft.

The approximate (spreadsheet) model is based on the assumption of a return to approximately normal depth within the reach between the entrances to successive inlets under all conditions. It is instructive to examine this assumption, using the differential model to provide a detailed computation of all parameters over the distance between inlets. Figure 24 depicts computations along a slope decreasing by 0.0001 for each barrier, as in the example problem presented above. The same circumstances of this example are employed here.

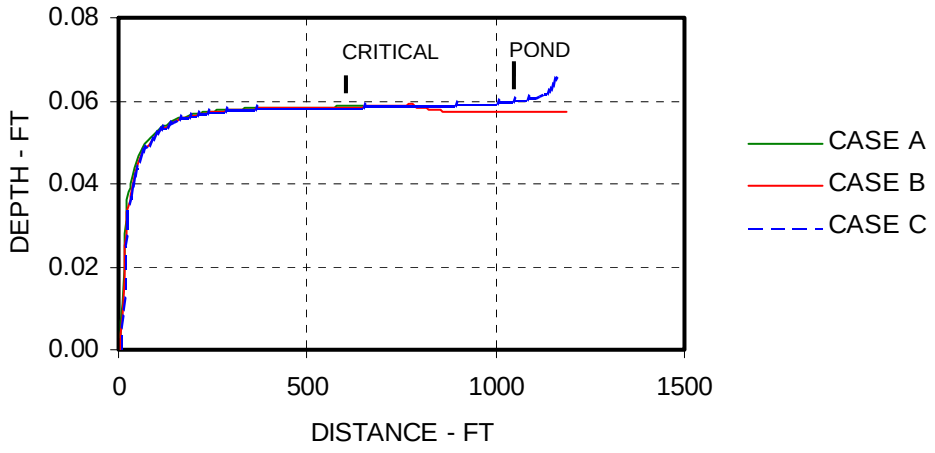

Figure 24: Comparison of detailed computational model with spreadsheet model for example problem in text. Case A: detailed model to first point of critical flow. Case B: spreadsheet model with critical depth for mild slope. Case C: spreadsheet model with normal depth assumption. Pond position indicated. Equilibrium depth is 0.057 feet.

Figure 24 presents a comparison between the detailed computational model and two versions of the spreadsheet model. Initially, the model results are virtually identical. The detailed model detects the first indication of the development of critical flow between inlets. Consequently, critical depth occurs earlier for this model and the computations are terminated. Cases B and C continue but each show results not much different than the equilibrium depth, indicating that the model is not very sensitive to the selection of normal or critical depth on mild slope.

CONCLUSIONS

1. The hydraulic performance of individual rectangular drain inlets formed in the base of concrete barriers has been measured for a range of typical pavement slope conditions. The results of this investigation confirm earlier reports that the depth of the approach flow near the inlet entrance could be used as a reliable predictor of discharge. An empirical correlation describing this relationship was obtained.

2. Methods for application of results obtained during this study to field installations have been presented. It is suggested that the simple correlation developed here be used to predict spread on slopes as well as inlet and bypass flow, by assuming that normal depth is attained just upstream of each inlet and ignoring any interaction between inlets. A weir flow correlation for discharge from ponds is also recommended.

3. A computational model suitable for evaluating barrier wall installations has been developed and tested. This model will predict conditions on grade and in depressed regions.

During this investigation several related questions not previously anticipated were raised. This discussion is intended to address at least in part some of these questions.

a) One obvious question is concerned with the applicability of these results to alternate configurations, specifically inlets which have a wider or narrower aperture (some states approve much wider inlets). The applicability of a linear transformation up or down appears to be justified by the scale tests made in this investigation. It is noted that this is not the same transformation discussed in Appendix C but rather a “distorted scale factor”. It is recommended that direct scale up of the results of this investigation be utilized until better information becomes available. The empirical correlation for inlet capacity under transverse flow does not scale with the inlet height.

b) A new design for barrier inlets is being implemented. This design consists of two inlets spaced closely together. As a first approximation these should be treated as per a) above, although because of the close spacing it is likely that some interference might be observed. At this time it is not know whether this may be constructive or destructive, but based on preliminary testing with inlet blocks there appears to be very little change in performance (cf. Appendix D).

c) Attention is called to the development of plastic, weighted barriers. For estimation and planning, it is realistic to treat these in the same manner as conventional concrete walls, with the possible exception of rounded edges. It was previously shown that this modification actually improves sump flow performance somewhat.

d) The performance of flooded inlets was not investigated during this study but as a recommendation, since under stagnant conditions the inlets behave as weirs and orifices; it is recommended that estimates could be made by using the same methods as common apertures are rated for flooded operation.

REFERENCES

1. Robinson, D.I., and McGhee, T.J., "Computer Modeling of Side-Flow Weirs", J.Irrigation and Drainage Engineering, Vol 119, No. 6, Nov./Dec. 1993

2. Singh, R. and Satyanarayana, T., "Automated Field Irrigation System Using Side Weirs", J. Irrigation and Drainage Engineering, Vol. 120, No. 1, Jan./Feb., 1994

3. Design Standards, Florida Department of Transportation, 2002.

4. Kranc, S. C., et al, Hydraulic Performance of Structures for Bridge Drainage , Report No. 747, Florida Department of Transportation, March 1997

5.Johnson, F. L. and Chang, F.M., Drainage of Highway Pavements HEC 12, FHWA, 1984.

6. S.C. Kranc, C.J. Cromwell and C.J. Rabens, "Hydraulic Capacity of Inertial Attenuators", presented at the Hydraulic Measurements and Experimental Methods Conference, ASCE /EWRI, in Estes Park, Colorado. July 28-31, 2002

7. Henderson, F.M., Open Channel Flow, Macmillan Co., New York, N.Y., 1966

APPENDIX A: NOTES TO ACCOMPANY SPREADSHEET SOFTWARE

1. This program functions like any conventional spreadsheet, load and operate in the normal fashion. Two versions have been provided, one allows for data entry of longitudinal slope and the other utilizes a vertical curve design program provided by FDOT.

2. Macros accompany this spreadsheet; when the initial enquiry regarding opening the sheet occurs, the option to enable should be chosen.

3. "Solver" must be available. If not on the current spreadsheet, this function can be added by following the directions (under "Tools/Add-ins").

4. Making an archival copy of this program on a separate disk is strongly suggested.

5. Although no regions or formulas are protected it is suggested that data entry changes be confined to the *yellow shaded regions only*. Modifying some other portion of the spreadsheet may have unintended consequences.

6. When entering data, note that the freeze pane feature is on and that the slider should be used to restore the full data column.

7. There is only one operation other than data entry, clicking the "SOLVE" button on the POND sheet. A background computation of the pond depth will be completed (if possible). There is no error trapping at this point and the user should try to cancel this operation. Do not use the Debug. For severe problems it may be necessary to reload from the archival copy.

8. The SOLVE operation takes some time (perhaps 15 seconds) to complete. Please make certain this operation is finished before proceeding.

9. The user should be aware that all software has the potential for error and no results can be guaranteed. Ultimately, all responsibility for application lies with the user.

APPENDIX B: FLOW IN GUTTERS AND INLETS

To analyze the information obtained during inlet capacity experiments. The pavement slope can be described by cross slope S_c and longitudinal slope S_0. For simplicity, it was assumed that the curb forms a 90° angle with the pavement so that a triangular section is formed with depth h, as shown in Figure 4. Because the cross slope is a small angle, the spread is approximately the same as the length across the pavement and the depth h, is very close to the measurement y, against the curb, as seen in the figure. Thus, the spread is approximately

$$T \approx \frac{y}{S_c} \tag{B-1}$$

The area is given approximately as

$$A \approx \frac{y^2}{2S_c} \tag{B-2}$$

The hydraulic radius is the same as the average depth

$$R_h \approx \frac{y}{2} \tag{B-3}$$

The flow velocity may be obtained from continuity and the total flow, Q_t

$$V \approx \frac{2Q_T S_c}{y^2} \tag{B-4}$$

The Froude number is defined in terms of the average depth

$$Fr \approx \left(\frac{8}{g}\right)^{1/2} \frac{Q_T S_c}{y^{5/2}} \tag{B-5}$$

The critical depth is

$$y_c \approx [\frac{8 Q_T^2 S_c^{\ 2}}{g}]^{1/5} \qquad \text{(B-6)}$$

The specific energy becomes

$$E \approx y + \frac{2 Q_T^2 S_c^2}{g y^4} \qquad \text{(B-7)}$$

From this point, a straightforward analysis of the frictional flow in the channel can be made however, it is often suggested that because the surface width of the flow is very large in comparison to depth, the standard formulation for a channel of triangular cross section is not completely satisfactory for predicting flow conditions and experimental evidence appears to confirm this discrepancy. An alternative formulation has been developed by integrating Manning's equation for infinitesimal rectangular elements of variable depth across the channel width, giving

$$Q_T \approx \frac{3 k S_c^{5/3} S_0^{1/2} T^{8/3}}{8 n} \qquad \text{(B-8)}$$

This formula yields results about 20% higher for the flow rate than that predicted by assuming a channel of triangular cross section. The normal depth associated with this formula is

$$y_n \approx [\frac{8 Q_T S_c n}{3 k S_0^{1/2}}]^{3/8} \qquad \text{(B-9)}$$

The flows must balance at the inlet. With subscripts T, I and B denoting total, inlet and bypass flow respectively,

$$Q_T = Q_I + Q_B \qquad \text{(B-10)}$$

An inlet efficiency is customarily defined as

$$e = \frac{Q_I}{Q_T} \tag{B-11}$$

Finally, under sump conditions the inlet flow is simply related to the depth y by

$$Q_I = C_{DW} L \sqrt{2g}\ y^{3/2} \tag{B-12}$$

where C_{DW} and C_{DO} are the discharge coefficients for both weir and orifice regime flows, respectively

$$Q_I = C_{DO} A \sqrt{2g}\ y^{1/2} \tag{B-13}$$

Here L is the width and A is the area of the opening.

APPENDIX C: SCALING RELATIONSHIPS

A generally accepted modeling technique for inlet flows requires that the Froude number of model and prototype are identical. The relationship between the velocities and discharge derive from this assumption and the length ratio $L_r = l_p/l_m$. Since the ratio of the depths is equal to the length ratio, from Equation B-5

$$\frac{Q_p}{Q_m} = L_r^{5/2} \qquad \text{(C-1)}$$

Using Equations B-2 and B-4 and applying continuity yields

$$\frac{V_m^2}{g y_m} = \frac{V_p^2}{g y_p} \qquad \text{(C-2)}$$

Applying the definition of the length ratio to the ratio of the Manning equations written for model and prototype (assuming identical slopes) results in

$$\frac{Q_p}{Q_m} = L_r^{8/3} \frac{n_m}{n_p} \qquad \text{(C-3)}$$

combining C-1 and C-3 yields

$$\frac{n_m}{n_p} = L_r^{-1/6} \qquad \text{(C-4)}$$

All transfer relationships for a scale factor of one-half are summarized in the table below.

SCALING RELATIONS FOR ONE-HALF SCALE MODEL

LINEAR DIMENSION	L_r	2.00
FLOW RATIO	Q_r	5.65
VELOCITY RATIO	V_r	1.41
ROUGHNESS RATIO	n_r	0.89

Since the correction for roughness indicated is typically small, no adjustments may be required in many cases.

APPENDIX D: AN APPROXIMATE MODEL FOR THE K- BARRIER

A new design for barrier inlets is currently being developed by the FDOT. This design consists of two inlets spaced closely together. As a first approximation the performance of these inlets should be treated as the conventional Index 415 above, although because of the close spacing it is likely that some interference might be observed. At this time it is not know whether this may be constructive or destructive, but based on preliminary testing with inlet blocks there appears to be very little change in performance.

In an attempt to provide a nondimensional representation of the capacity of an inlet with transverse, supercritical flow, the following relationship was introduced earlier

$$\frac{Q_I}{g^{1/2}H^{5/2}} = 4.16\frac{y}{H} - 0.92 \qquad \text{(D-1)}$$

Although written in nondimensional form, this statement does not imply that scaling is appropriate. Here the H dimension was 0.167ft. For a 2% typical cross slope the spread expected if the aperture was submerged would be 0.167/.02=8.33 ft, probably too large to be practical. In other words, it is unlikely that the inlets would be submerged except possibly a large compound cross slope. It is believed that the relationship above is conservative in estimate of capacity. It is noted in passing that this straightline relationship predicts negligible flow at a shallow water depth. Although this may a realistic approximation, it is likely that in reality the linear trend shifts for shallow conditions and approaches zero for zero depth.

The following approach is suggested for estimating the capacity of the K barrier. Rewriting the expression above to give a dimensional capacity,

$$Q_I = g^{1/2}H^{5/2}(4.16\frac{y}{H} - 0.92) \qquad \text{(D-2)}$$

where H= 0.167ft. This relationship becomes

$$Q_I = 1.606\,y - 0.059 \qquad \text{(D-3)}$$

Where y is measured in feet and Q in CFS. This relationship, originally constructed for an opening of 2.58 ft, is assumed to apply to another opening L (so long as L is not very much larger or smaller than the original specification. In the case of the K barrier, the vertical dimension is 0.25 ft, and the horizontal

opening is 1.5 ft, so it may be assumed that the water would not cover the inlet under practical circumstances and an appropriate new relationship for the K-type barrier would be

$$Q_I = (1.606\,y - 0.059)\,\frac{1.5}{2.58} \qquad \text{(D-4)}$$

or

$$Q_I = 0.934\,y - 0.034 \qquad \text{(D-5)}$$

for each inlet.

Detailed modeling was applied to the case of the K-barrier on a constant steep slope. Computations for the reach between both the widely spaced inlets and the closely spaced inlets indicated that the assumption of normal depth was still a conservative statement and should be satisfactory for the evaluation program.

APPENDIX E: COMPOSITE SLOPES

Following the methods used to derive the discharge relationship for a shallow triangular channel, the flow area is divided into small, nearly rectangular sections having an area equal to hdx where h is the local depth. The wetted perimeter is approximately dx, so that hydraulic radius is approximately h. Thus the flow rate is given by (English units)

$$Q = \int_0^{y_n} \frac{1.49 S_0^{1/2}}{n S_x} h^{5/3} dh \qquad \text{(E-1)}$$

when $dx=h/S_x$ is substituted. Integrating yields Eqn

$$Q = \frac{3}{8} \frac{1.49 S_0^{1/2}}{n S_x} y_n^{8/3} \qquad \text{(E-2)}$$

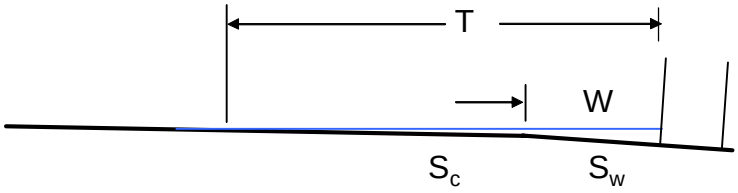

A similar treatment for a composite slope yields the following:

$0<y_n<WS_W$

$$Q = \frac{3}{8} \frac{1.49 S_0^{1/2}}{n S_w} y_n^{8/3} \qquad \text{(E-3)}$$

$WS_W < y_n$

$$Q = \frac{3}{8} \frac{1.49 S_0^{1/2}}{n S_x} (y_n - WS_w)^{8/3} + \frac{3}{8} \frac{1.49 S_0^{1/2}}{n S_w} y_n^{8/3} - \frac{3}{8} \frac{1.49 S_0^{1/2}}{n S_w} (y_n - WS_w)^{8/3} \qquad \text{(E-4)}$$

This function must be tabulated for an appropriate range of y_n then inverse interpolation can be used to compute y_n as a function of Q. Other approaches to calculating capacities of composite channels are also possible.

In the same manner, the critical depth and the Froude number must be calculated by formula and related to the depth and flow conditions. The following formulas apply:

$$Fr^2 = \frac{Q^2 T}{gA^3} \qquad \text{(E-5)}$$

For $0<y<WS_W$, the spread T is given by y/Sc and the area by Ty/2. For $WS_W<y$, the spread is

$$T = W + \frac{y - WS_w}{S_C} \qquad \text{(E-6)}$$

and the area is

$$A = WS_w / 2 + (y - WS_w) + (T - W)(y - WS_w)/2 \qquad \text{(E-7)}$$

The critical depth, $y_{c,}$ is obtained by finding that depth for which the Froude number is unity at some Q.

APPENDIX F: DEVELOPMENT OF A VISUAL BASIC PROGRAM

As part of an extended effort associated with this research, a next generation design program, written in Visual Basic was developed and delivered to the FDOT under separate cover, along with a tutorial instruction manual to accompany the program.. This appendix summarizes the assumptions leading to this model.

A goal of this part of the effort was to develop a program that accepts input information about the wall installation on the pavement, identifies a circumstance of interest (such as pond formation), calculates flow at any point along the wall, and identifies possible spread problem areas. The program was based on the following simplifying assumptions and information gained from the results from more detailed analyses.

1. The assumption of flow slightly greater than normal flow for a simple triangular channel (as discussed previously) will be utilized. About 22% greater flow in the channel is predicted and is therefore conservative.

2. For supercritical flow on steep slopes it will be assumed that the depth of water in the channel returns to local normal depth (as conventionally defined) just upstream of the inlet for Froude number is greater than about 1.2. For values of Fr below 1.2 (but above 1.0) the average of critical depth and normal depth will be used to predict discharge. Detailed modeling indicates that this assumption is conservative.

3. For situations where the slope is decreasing along the flow direction, when the condition of critical flow at the entrance to an inlet is first detected, subcritical flow will be assumed to be the flow state. For subcritical flow on mild slopes the depth of the water at the inlet entrance is assumed to be critical (free flow into inlet).

4. For situations where the longitudinal slope varies, the change will be assumed to be incremental at inlets and the slope will be constant between inlets.

5. For all conditions with transverse flow across the inlet, capacity is assumed to be given by the empirical relation developed in the experimental investigation for both mild and steep slopes (flow rate determined as a function of depth at the upstream edge). Since stagnant conditions result in much higher inlet flow, this assumption appears conservative.

6. The transition from steep to mild slope means that the flow will change from a supercritical condition to a subcritical state. Because the slope

changes gradually, this transition occurs near Fr=1.0 and corresponds to a very weak hydraulic jump. In fact, the jump may be dispersed over an extended reach with regions of mixed flow. Changes in specific energy due to a transition from supercritical to subcritical flow between inlets will be neglected.

7. To locate possible transitions from flow on grade to a pond (stagnant) condition, the pond depth necessary to produce a flow balance into and out of the pond is calculated. The extent of the pond along the slope can then be determined. The calculation of spread on the grade is then merged smoothly with the spread due to the pond. The true situation is more complex but this assumption should be an acceptable compromise. The possibility that such a transition might occur right at an inlet is ignored. It is most likely that the flow into the pond is subcritical.

8. For stagnant conditions, inlet flow is evaluated by other empirical relations for orifice and weir flow developed here and elsewhere, based on the local depth in the pond behind the inlet.

9. To account for the effect of trash accumulation at the inlets, an assumption made here is to scale the capacity of the aperture with the fractional blockage. It is noted that this relationship has not been verified and may not be valid, especially at elevated levels of accumulation.

10. Although the program has the ability to treat point discharges, there are practical limitations to the quantity of flow that may be added to the channel. It is suggested that point discharges not exceed a few times the equilibrium flow in the channel. Large discharges may result in an unacceptable local spread.